International Telecommunication Union

ITU-R
Radiocommunication Sector of ITU

Report ITU-R BT.2209-1
(05/2013)

Calculation model for SFN reception and reference receiver characteristics of ISDB-T system

BT Series

Broadcasting service
(television)

Foreword

The role of the Radiocommunication Sector is to ensure the rational, equitable, efficient and economical use of the radio-frequency spectrum by all radiocommunication services, including satellite services, and carry out studies without limit of frequency range on the basis of which Recommendations are adopted.

The regulatory and policy functions of the Radiocommunication Sector are performed by World and Regional Radiocommunication Conferences and Radiocommunication Assemblies supported by Study Groups.

Policy on Intellectual Property Right (IPR)

ITU-R policy on IPR is described in the Common Patent Policy for ITU-T/ITU-R/ISO/IEC referenced in Annex 1 of Resolution ITU-R 1. Forms to be used for the submission of patent statements and licensing declarations by patent holders are available from http://www.itu.int/ITU-R/go/patents/en where the Guidelines for Implementation of the Common Patent Policy for ITU-T/ITU-R/ISO/IEC and the ITU-R patent information database can also be found.

<div style="border:1px solid">

Series of ITU-R Reports

(Also available online at http://www.itu.int/publ/R-REP/en)

Series	Title
BO	Satellite delivery
BR	Recording for production, archival and play-out; film for television
BS	Broadcasting service (sound)
BT	**Broadcasting service (television)**
F	Fixed service
M	Mobile, radiodetermination, amateur and related satellite services
P	Radiowave propagation
RA	Radio astronomy
RS	Remote sensing systems
S	Fixed-satellite service
SA	Space applications and meteorology
SF	Frequency sharing and coordination between fixed-satellite and fixed service systems
SM	Spectrum management

</div>

Note: This ITU-R Report was approved in English by the Study Group under the procedure detailed in Resolution ITU-R 1.

REPORT ITU-R BT.2209-1

**Calculation model for SFN reception and reference
receiver characteristics of ISDB-T system**

(2010-2013)

TABLE OF CONTENTS

Summary

This Report provides detailed considerations on receiver characteristics under single frequency network (SFN) conditions for ISDB-T system. It introduces new technical parameters that dominate receiver performances, in addition to the conventional planning parameters. The new parameters are amplitude proportional noise (APN), FFT window setting margin and interpolation filter characteristics used for reference carrier recovery. Using these parameters, the overall receiver characteristics can be expressed by a single parameter called guard interval mask characteristics, which is useful in estimating whether or not the signal is received correctly.

Furthermore, the Report gives a reference receiver characteristic that would be applied in frequency planning and/or network design of ISDB-T based broadcasting systems. The calculation method for SFN reception and the reference receiver characteristics have been established in ARIB TR-B14, which is successfully applied in planning and designing of broadcasting networks in Japan.

It is shown that SFN does not work unconditionally and works well only when the reception signals are kept under certain conditions in terms of reception voltages, desired to undesired ratios (DURs), delays between main and SFN signals and so on.

Chapter I

SFN with delays less than guard interval duration

First we will derive the condition that gives single frequency network (SFN) failure when a single SFN wave exists. Then, we will discuss about the conditions when multiple SFN waves exist. Also we will give some considerations on the receiver characteristics that are necessary to estimate the area of failure. We call SFN with delays less than guard interval duration as "inner-GI SFN" in short.

1   In the case of a single SFN wave

The received signal exhibits ripples in frequency response when a desired signal is received with SFN waves. In this case, the bit error rates (BER) of the OFDM carriers positioned at peaks in frequency response becomes better, because the input signal levels are high for those carriers. On the other hand, the BER of the carriers positioned at dips in frequency response become worse because the input levels are low. We can estimate the occurrence of SFN failure by calculating the BERs for every carrier and summing up them to check whether or not the total BER is worse than the required value.

Figure 1 shows an example of frequency response of received signal. Figure 1a is the case where the desired signal is just at the level that gives the required carrier-to-noise ratio (CNR). In this example, we assume the total BER being worse than the required value, as there are many carriers of which BER is worse than the reference value. If we increase the levels of both desired and SFN signals, the number of carriers having worse BER is decreased, and then the signal is correctly received, as shown in Fig. 1b. The SFN failure takes place depending not only on the desired to undesired ratios (DUR) but also on the levels of the received signal itself.

FIGURE 1
Example of received signal
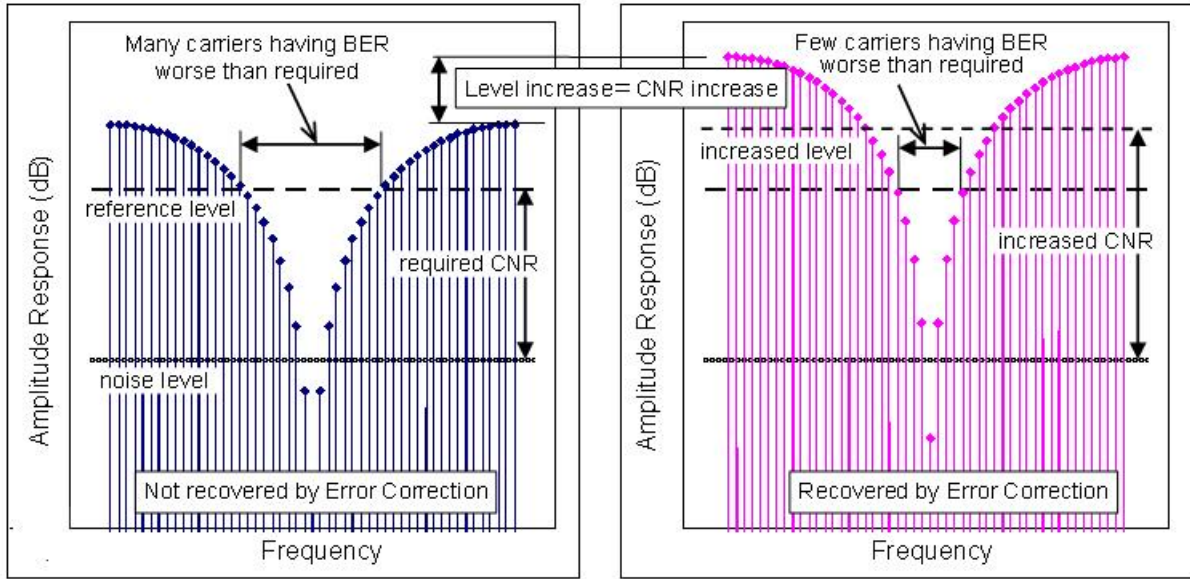
a) in the case of reference signal level   b) in the case of signal level increased

1.1 Mathematical equations used in this text

The relationship between BER and CNR are as follows:

for QPSK

$$BER = \frac{1}{2} Erfc\left(\sqrt{\frac{1}{2}\frac{C_p}{N_p}}\right) \quad \text{and} \quad \frac{C_a}{N_a} = \sqrt{\frac{C_p}{N_p}} = \sqrt{2} \cdot Erfc^{-1}(2 \cdot BER) \tag{1}$$

for 16-QAM

$$BER = \frac{3}{8} Erfc\left(\sqrt{\frac{1}{10}\frac{C_p}{N_p}}\right) \quad \text{and} \quad \frac{C_a}{N_a} = \sqrt{\frac{C_p}{N_p}} = \sqrt{10} \cdot Erfc^{-1}\left(\frac{8}{3} \cdot BER\right) \tag{2}$$

for 64-QAM

$$BER = \frac{7}{24} Erfc\left(\sqrt{\frac{1}{42}\frac{C_p}{N_p}}\right) \quad \text{and} \quad \frac{C_a}{N_a} = \sqrt{\frac{C_p}{N_p}} = \sqrt{42} \cdot Erfc^{-1}\left(\frac{24}{7} \cdot BER\right) \tag{3}$$

where:

C_p: average power of signal

C_a: *r.m.s.* amplitude of signal

N_p: noise power

N_a: *r.m.s.* amplitude of noise

and $Erfc(x) = \frac{2}{\sqrt{\pi}} \int_x^\infty \exp(-t^2) dt$.

The relationship between the *Erfc* above and *Ndist* (normal distribution function) generally used in mathematics is as follows:

$$Ndist(x) = \frac{1}{\sqrt{2\pi}} \int_{-\infty}^{x} \exp\left(-t^2/2\right) dt$$

$$\begin{aligned} Erfc(x) &= \frac{2}{\sqrt{\pi}} \int_{x}^{\infty} \exp\left(-t^2\right) dt \\ &= \frac{2}{\sqrt{\pi}} \int_{\sqrt{2}\,x}^{\infty} \exp\left(-u^2/2\right) \frac{du}{\sqrt{2}} = 2 \frac{1}{\sqrt{2\pi}} \int_{\sqrt{2}\,x}^{\infty} \exp\left(-u^2/2\right) du \\ &= 2 \cdot Ndist\left(-\sqrt{2}\,x\right) \end{aligned} \tag{4}$$

where:

$$u: \quad \sqrt{2}\,t\,.$$

The relationship between the inverse functions of the above is:

$$\begin{aligned} P &= Erfc(x) = 2 \cdot Ndist\left(-\sqrt{2}x\right) \\ \frac{P}{2} &= Ndist\left(-\sqrt{2}\,x\right) \;\Rightarrow\; x = \frac{-1}{\sqrt{2}} Ndist^{-1}\left(\frac{P}{2}\right) \\ \therefore\;\; Erfc^{-1}(P) &= \frac{-1}{\sqrt{2}} Ndist^{-1}\left(\frac{P}{2}\right) \end{aligned} \tag{5}$$

1.2 Note to CNR used in theoretical calculation

Recommendation ITU-R BT.1368 defines reference CNRs for various modulations and forward error correction (FEC) code rates, where the carrier level is expressed by the power of the transmission signal that contains several kinds of information, such as scattered pilots (SP), system controls, in addition to content signals. In the following theoretical calculation, we will deal with content signals only and will apply the reference CNRs being a little different from those in the Recommendation.

To keep consistency among various modulations, we define the reference symbol error rate (SER) that gives the required BER for each FEC, and we assume the reference SER is unchanged among modulations. The reference CNRs are then derived from the reference SERs under additive white Gaussian noise environment. Table 1 shows the reference SERs and CNRs applied in this Report.

TABLE 1

Reference SER and CNR applied in theoretical calculation

	FEC=1/2	FEC=2/3	FEC=3/4	FEC=5/6	FEC=7/8
Reference SER	5.0×10^{-2}	2.5×10^{-2}	1.3×10^{-2}	6.0×10^{-3}	3.0×10^{-3}
QPSK	4.3 dB	5.8 dB	6.9 dB	8.0 dB	8.8 dB
16-QAM	10.5 dB	12.3 dB	13.4 dB	14.6 dB	15.5 dB
64-QAM	15.9 dB	17.9 dB	19.2 dB	20.5 dB	21.4 dB

1.3   Increase in the required CNR

In the case of a single SFN wave, the frequency response of the received signal is given by equation (6).

$$F_a(\omega) = \sqrt{1 + U_a^2 + 2U_a \cdot \cos(\omega \cdot \tau)} \tag{6}$$

where:

  U_a: amplitude of SFN wave relative to desired wave

  τ: delay of SFN signal.

Figure 2 shows examples of the increase in the required CNR when an SFN wave exists. The horizontal axis of the graphs denotes the power of SFN wave relative to the desired signal, that is, the inverse figures of DUR. The vertical axis denotes the increase in the required CNR. The actual values of CNR necessary for correct reception are obtained by adding these increases to the reference CNR such as 19.2 dB for 64-QAM-FEC3/4, 21.4 dB for 64-QAM-FEC7/8, and so on. The curves in Fig. 2 are obtained by calculating the CNR that gives BER of 1.3×10^{-2} for FEC3/4 or 3.0×10^{-3} for FEC7/8 against a number of SFN waves of which amplitude, delay and phase are given randomly. The relationships given by these curves are called "CNR Increase Functions" in this document.

Since CNR Increase Function cannot be expressed by simple mathematical formula, we introduce approximated function for it, as below:

$$
\begin{aligned}
CN_{up}(U\mathrm{dB}) &= \alpha \cdot \exp\left[-\left|\beta \cdot U\mathrm{dB}\right|^{\gamma}\right] && (U\mathrm{dB} \le 0) \\
&= \alpha \cdot \exp\left[-\left|\beta \cdot U\mathrm{dB}\right|^{\gamma}\right] - U\mathrm{dB} + A \cdot U\mathrm{dB} && (U\mathrm{dB} > 0)
\end{aligned}
\tag{7}
$$

where:

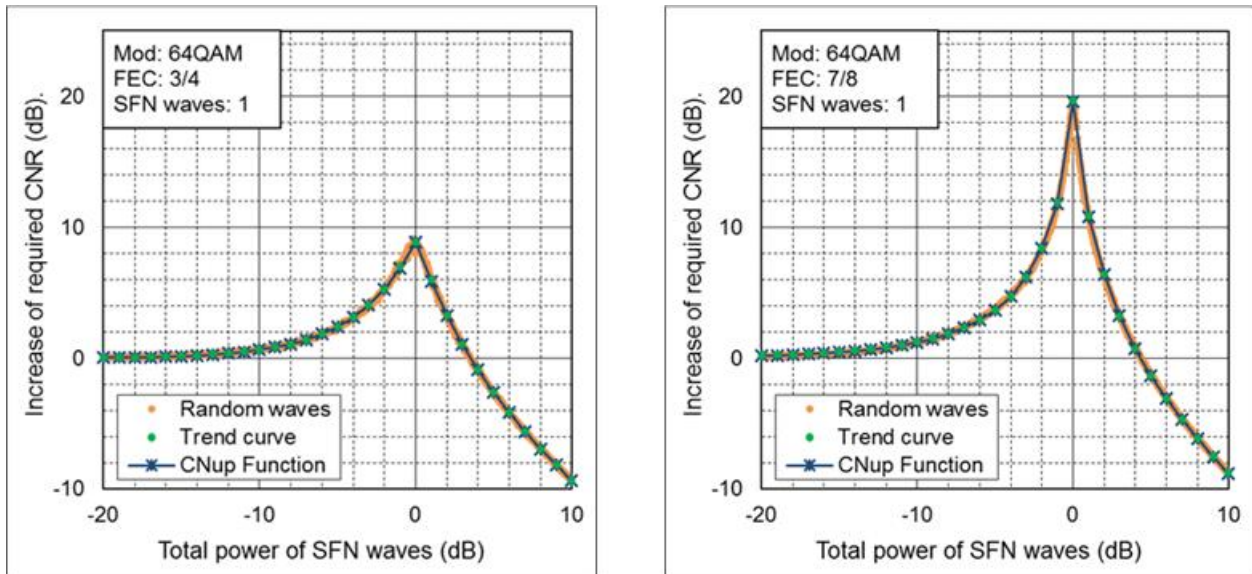 $U\mathrm{dB}$:   denotes power of SFN wave expressed (dB)

  $CN_{up}(U\mathrm{dB})$:   denotes increase in required CNR expressed (dB).

The values of the coefficients, α, β, γ and A are given in Table 2.

FIGURE 2

Example of increase in the required CNR

a) FEC = 3/4   b) FEC = 7/8

TABLE 2

Coefficient for CNR Increase Function

Coefficient	Modulation	FEC:7/8	FEC:5/6	FEC:3/4	FEC:2/3	FEC:1/2
α	64-QAM	19.653	14.562	8.915	4.915	1.207
	16-QAM	21.534	16.384	10.611	6.493	2.388
	QPSK	23.722	18.503	12.624	8.380	3.990
β	64-QAM	0.4013	0.3259	0.2605	0.2197	0.1498
	16-QAM	0.4335	0.3510	0.2784	0.2361	0.1827
	QPSK	0.4740	0.3828	0.3015	0.2550	0.2086
γ	64-QAM	0.7362	0.8442	1.0071	1.1573	1.5873
	16-QAM	0.7038	0.8018	0.9529	1.0932	1.3242
	QPSK	0.6704	0.7578	0.8946	1.0252	1.2018
A	64-QAM	1.025	0.854	0.662	0.502	0.356
	16-QAM	1.072	0.913	0.722	0.559	0.411
	QPSK	1.125	0.985	0.786	0.633	0.466

NOTE – A = 0 for single SFN wave condition (see § 2.1 for multiple SFN waves condition).

The value of α corresponds to the maximum increase of required CNR, which takes place at DUR = 0 dB. A large difference is found in the maximum CNR increase between FEC 3/4 and 7/8, comparing to 2-3 dB in the case without SFN waves. This difference must be noted in broadcasting network design, in other words, FEC 7/8 could not be applied in the actual world where SFN is more or less used.

1.4   Noise characteristics in receivers

The noise that affects reception performance can be summarized in two categories; one is the noise of which amplitude is independent of the input signal, such as thermal noise, and the other is the noise of which amplitude increases/decreases according to the input signal level. The former is called "fixed noise" and the latter "amplitude proportional noise" (APN) in this text.

Fixed noise consists of thermal noise, man-made noise, noise figure of receivers, and so on. An example of link budget reported by the National Council on Information and Telecommunication in Japan applies thermal noise of 300 K, man-made noise of 700 K, and noise figure of 3 dB. The value of fixed noise is estimated to be 8.5 dB(μV) (@75Ω) in this case.

Amplitude proportional noise is mainly determined by receiver characteristics, such as quantization noise of A/D conversion, clipping noise, phase jitter of local oscillator.

The words "fixed" and "amplitude proportional" come from the features of noise when expressed equivalently at the receiver input terminal.

1.4.1   Clipping noise

Since the amplitude distribution of OFDM signal exhibits a normal distribution, an enormous dynamic range is required for receivers to treat the signal without distortions. Normal receivers clip the signals exceeding a certain level, and generate clipping noise in some extent.

Figure 3 explains clipping. The clipped waveform is equivalent to the input waveform with adding the signal components that exceed the clipping level in the opposite polarity. The component that exceeds the clipping level has a pulse waveform, as shown in the figure.

The probability that an OFDM signal takes a level of x is written by $Gauss(x/S_{rms})$, where S_{rms} denotes *r.m.s.* amplitude of the signal, and $Gauss(*)$ probability density function of a normal distribution. The amplitude of the pulse component that exceeds the clipping level is written by $(x - CL)$, where CL denotes the clipping level.

Using the above, we can estimate the power of the pulses or clipping noise as below:

$$NP_{clip} = \int_{CL/S_{rms}}^{\infty} (x - CL)^2 \cdot Gauss\left(x/S_{rms}\right) dx \qquad (8)$$

The spectrum of clipping noise can be regarded as flat noise, because the intervals of these pulses are considerably large and isolated pulse has flat spectrum.

FIGURE 3

Clipping noise
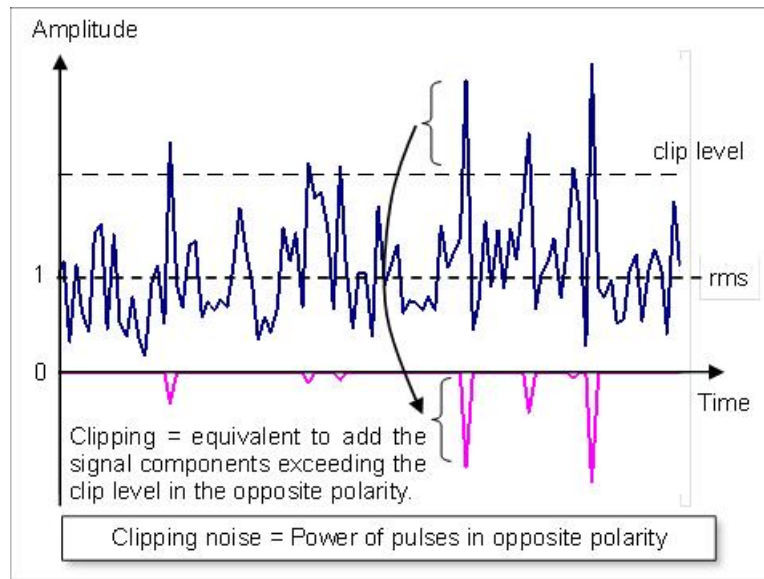
1.4.2 Quantization noise of A/D conversion

It is assumed for normal receivers that the clipping level is set equal to the full scale of the A/D converter. Then, the quantization noise is given by the well-known equation (9).

$$NP_{adc} = LSB^2 / 12$$
$$= \left(CL \cdot 2^{-N}\right)^2 / 12 = CL^2 \cdot 2^{-2N} / 12 \tag{9}$$

where:

 LSB: denotes the amplitude of the least significant bit

      N: denotes the bit-length of A/D converter.

The noise power given by equations (8) and (9) is in proportion to square of clipping level, that is, the amplitude of the noise is in proportion to the clipping level. As the receivers usually adjust the signal amplitude by AGC to a certain level corresponding to the clipping level, we can regard these noises to be in proportion to the input signal level.

Figure 4 shows examples of amplitude proportional noise. It is seen from the figure that the clipping level should be set at approximately 4 times (+12 dB) the *r.m.s.* signal amplitude and that the optimum clipping level depends on the bit-length of A/D conversion.

FIGURE 4

Amplitude proportional noise
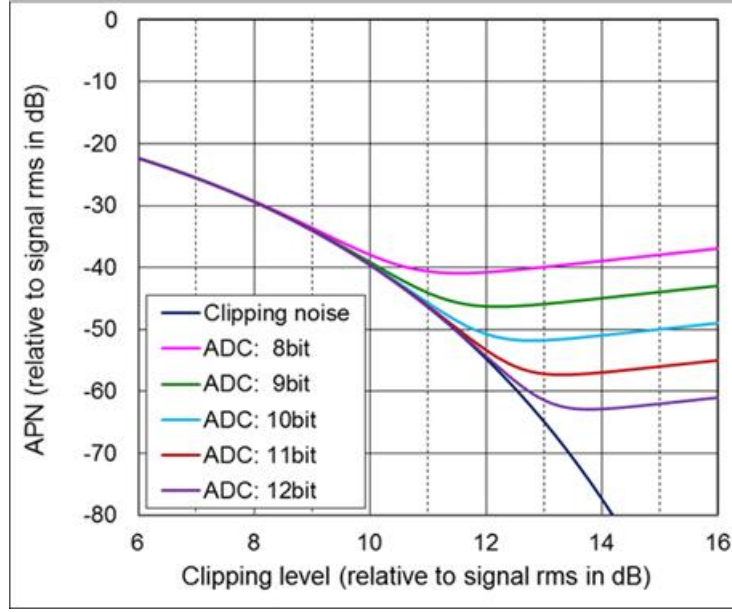
1.4.3 Other amplitude proportional noises

There are a lot of amplitude proportional noise sources other than described above, such as phase jitter of PLL, computational errors, and so on. In addition, transmitted signals include APN such as intermodulation components generated in the transmitter power amplifiers, noises included in the transmitter input signal (in the case of relay stations with broadcasting wave relay), etc. We can treat these transmitter noises to be equivalently generated in the receiver, and we will express the APN including all noise sources in a single value relative to the *r.m.s.* amplitude of the input signal.

1.5 Conditions that gives SFN failure

Now we will express the factors that are used in the digital reception estimation. They are:

$$CN = CN_0 \times CN_{up}\left(U_{rms}/D_{rms}\right)$$
$$NP = NP_{fix} + NP_{amp}\left(S_{rms}\right) \tag{10}$$
$$S_{rms} = \sqrt{D_{rms}^2 + U_{rms}^2}$$

where:

CN:	required CNR when SFN wave exists
CN_0:	required CNR without SFN waves
$CN_{up}(*)$:	CNR Increase Function defined by equation (7)
U_{rms}:	*r.m.s.* amplitude of SFN wave
D_{rms}:	*r.m.s.* amplitude of desired wave
S_{rms}:	*r.m.s.* amplitude of the input wave composed of desired and SFN waves
NP:	sum of fixed noise and amplitude proportional noise
NP_{fix}:	noise power of fixed noise
$NP_{amp}(*)$:	noise power of amplitude proportional noise expressed as a function.

When the received signal is higher by CN times the noise power calculated by equation (10), the digital signal is correctly received, as the CNR of the received signal being higher than the required

one. On the contrary, when the signal is lower than CN times the noise power, the digital signal cannot be correctly received, as the CNR of the received signal is lower than the required one. Hence, the condition that gives SFN failure can be obtained by resolving the following equation:

$$D_{rms}^2 = CN \times NP$$
$$= CN_0 \cdot CN_{up}\left(U_{rms}/D_{rms}\right) \times \left\{ NP_{fix} + NP_{amp}\left(\sqrt{D_{rms}^2 + U_{rms}^2}\right)\right\} \tag{11}$$

Figure 5 shows examples of SFN failure conditions calculated by equation (11) in the case of APN of −40 dB. The area surrounded by the pink curve represents the conditions that give SFN failure. In the case of FEC 3/4, SFN failure does not take place even at the worst case of DUR = 0 dB when the desired signal is higher than a certain level, while in the case of FEC 7/8, it occurs around DUR = 0 dB regardless of the desired signal level.

FIGURE 5

Example of SFN failure conditions (64-QAM, APN = −40 dB)
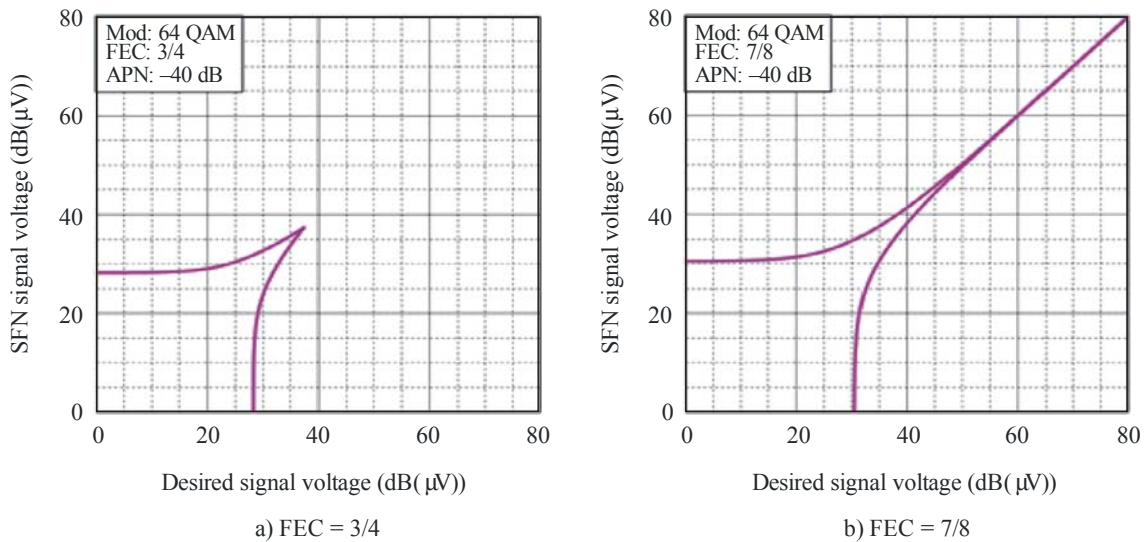

a) FEC = 3/4

b) FEC = 7/8

Report BT.2209-05

Figure 6 shows examples of SFN failure in the case of APN of −28 dB. In this case, the failure takes place just on the condition of DUR = 0 dB even with FEC 3/4. The range of DUR that generates SFN failure becomes wider with FEC 7/8. The SFN failure conditions thus depend on the FEC applied as well as on the APN, which is one of the receiver characteristics to be specified.

Example of SFN failure conditions (64-QAM, APN = –28 dB)

a) FEC = 3/4   b) FEC = 7/8
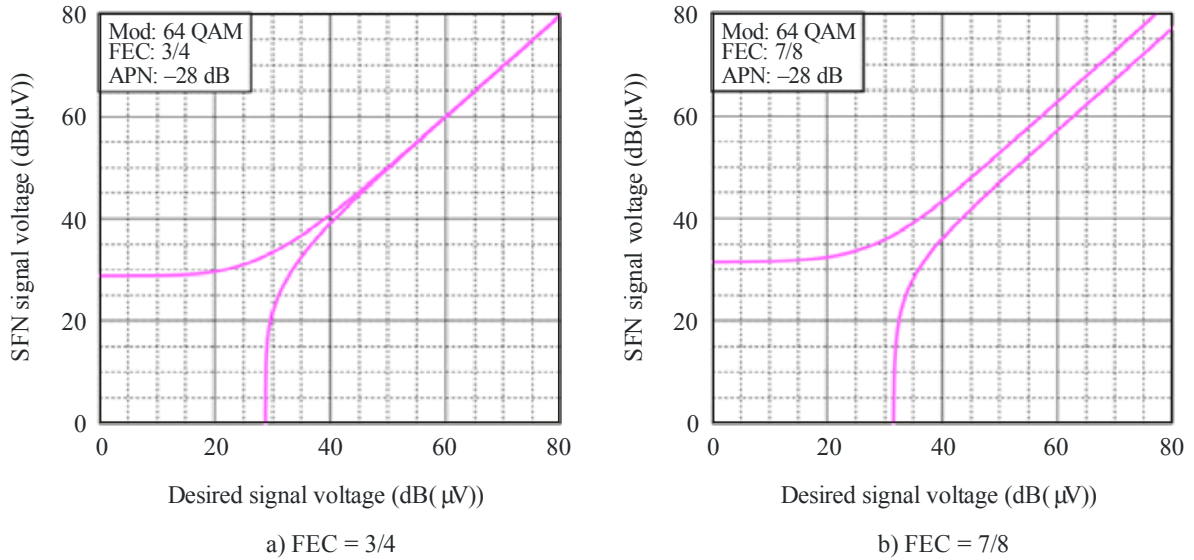
1.6   SFN non-failure conditions

It is attractive that there exist conditions without SFN failure, as shown in Fig. 5. We will give considerations on which conditions SFN failure does not occur. We will take into account APN only, since the conditions without SFN failure are limited in the high signal voltage range in which fixed noise can be neglected. The maximum increase in the required CNR takes place at DUR = 0 dB, as shown in Fig. 2, and the value is equal to α in Table 2.

For example, the required CNR is calculated to be 28.1 dB by adding the CNR increase of 8.9 dB to the reference CNR of 19.2 dB in the case of 64-QAM-FEC3/4, and it is 41.1 dB (increase of 19.7 dB + reference of 21.4 dB) in the case of 64-QAM-FEC7/8.

The input signal level is 3 dB higher compared to the desired signal when DUR = 0 dB, and hence, the APN is also larger by 3 dB. Then we will obtain the conditions for SFN non-failure when the desired signal is higher than this increased CNR.

$$NP_{amp} \leq -\left(CN_0 + CN_{up}(\max) + 3\right) = -\left(CN_0 + \alpha + 3\right) \qquad \text{dB} \qquad (12)$$

It can be derived by resolving equation (12) that SFN non-failure conditions require the APN being less than –30.3 dB for 64-QAM-FEC3/4 and –44.8 dB for 64-QAM-FEC7/8.

It is seen in Fig. 4 that the APN of –35 dB can be realized with an 8-bit A/D converter, and that 10-bit or more is required to obtain APN of –45 dB. It may be difficult to realize APN to be less than –45 dB when taking into account the other noise sources such as jitter of PLL, etc. Thus, it depends on the receiver performance whether or not the SFN failure takes place and we have to specify the reference receiver characteristics to be used in the broadcasting network design.

1.7   Location variation

If we can predict accurate values of field strength of the desired and SFN waves, we can estimate whether or not SFN failure takes place at the location concerned, by applying equation (12) and/or Fig. 5. However, we introduce a statistical method, because it is impossible to predict accurate field strengths.

Here we assume the mean and standard deviation of a field strength distribution in the area concerned to be μ_x and σ_x respectively for the desired wave, and those for the SFN wave to be μ_y and σ_y. Further assuming the correlation between the desired wave and the SFN wave to be ρ, then we can express the probability density of field strengths as follows:

$$F(E_x, E_y) = \frac{1}{2\pi\sqrt{A}} \exp\left[-\left\{ a_{11}(E_x - \mu_x)^2 + 2a_{12}(E_x - \mu_x)(E_y - \mu_y) + a_{22}(E_y - \mu_y)^2 \right\} \right]$$ (13)

where, $A = \sigma_x^2 \sigma_y^2 (1 - \rho^2)$, $\quad a_{11} = \sigma_y^2 / A$, $\quad a_{12} = -\rho\, \sigma_x \sigma_y / A$, $\quad a_{22} = \sigma_x^2 / A$

We can calculate the probability of SFN failure occurrence at a particular location by integrating equation (13) over the conditions that give SFN failure. Then the probability of SFN failure occurrence is written by equation (14).

$$P(\mu_x, \mu_y) = \iint\limits_{\text{SFN failure conditions}} F(E_x, E_y)\, dE_x\, dE_y$$ (14)

Figure 7 shows the calculation results of equation (14) for 64-QAM-FEC3/4 and for 64-QAM-FEC7/8, respectively. The probability of the failure for 64-QAM-FEC3/4 is almost zero in the region of received voltage being higher than 40 dB(μV), while it remains at 10-20% even in high reception voltage regions for 64-QAM-FEC7/8.

We apply equation (14) as the basic algorithm of "digital reception simulator", which is used in the channel plan calculation, especially for small-scale transmission stations.

FIGURE 7

Example of probability of SFN failure occurrence (64-QAM)
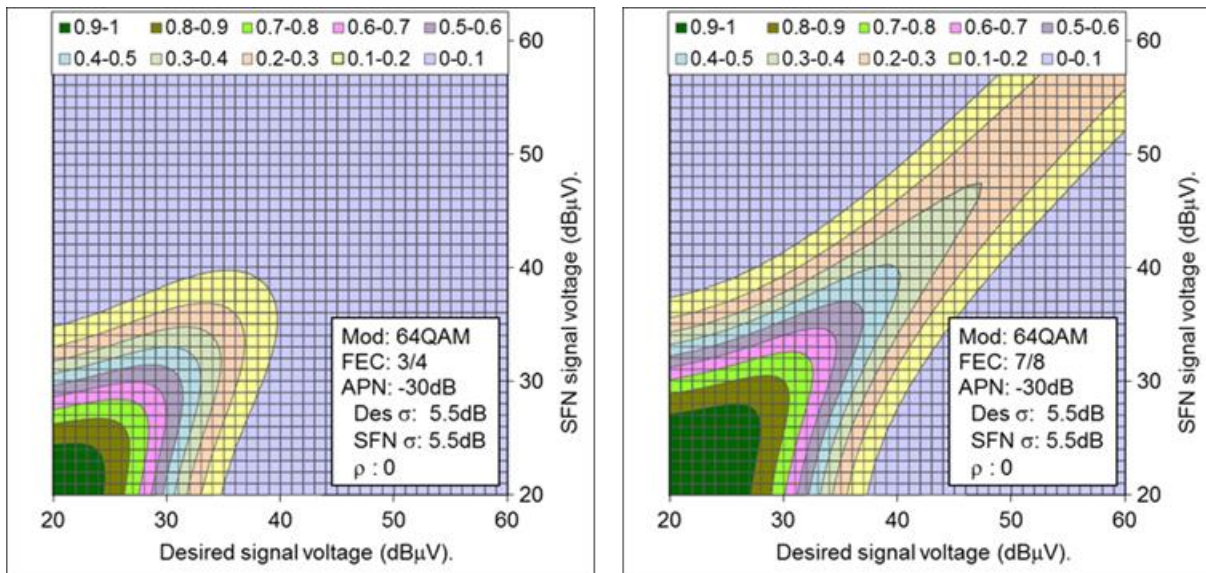
a) FEC = 3/4

b) FEC = 7/8

1.8 Location correlation

The field strength distributions of the desired and SFN waves can be assumed to exhibit the same statistics in each other, even if they come from different directions. Recommendation ITU-R P.1546 describes the standard deviation of field strengths for digital broadcasting waves to be 5.5 dB. Considering that the field strength distribution is caused mainly by clutters near the reception point, such as terrain, trees, buildings, etc. field strengths seem to have correlation between the desired and SFN waves. For example, field strengths would be lower at a hollow in the ground regardless of

wave directions, or they would be higher at a top of hill. The correlation would be stronger with closer the directions.

Figure 8 shows changes in the probability of SFN failure occurrence by the correlation ρ. We will apply ρ = 0 as the most general condition, although the appropriate values differ from one reception location to another.

FIGURE 8

**Changes in probability of SFN failure by location correlation**

a) correlation = 0

b) correlation = 0.5

c) correlation = 0.7

d) correlation = 0.9
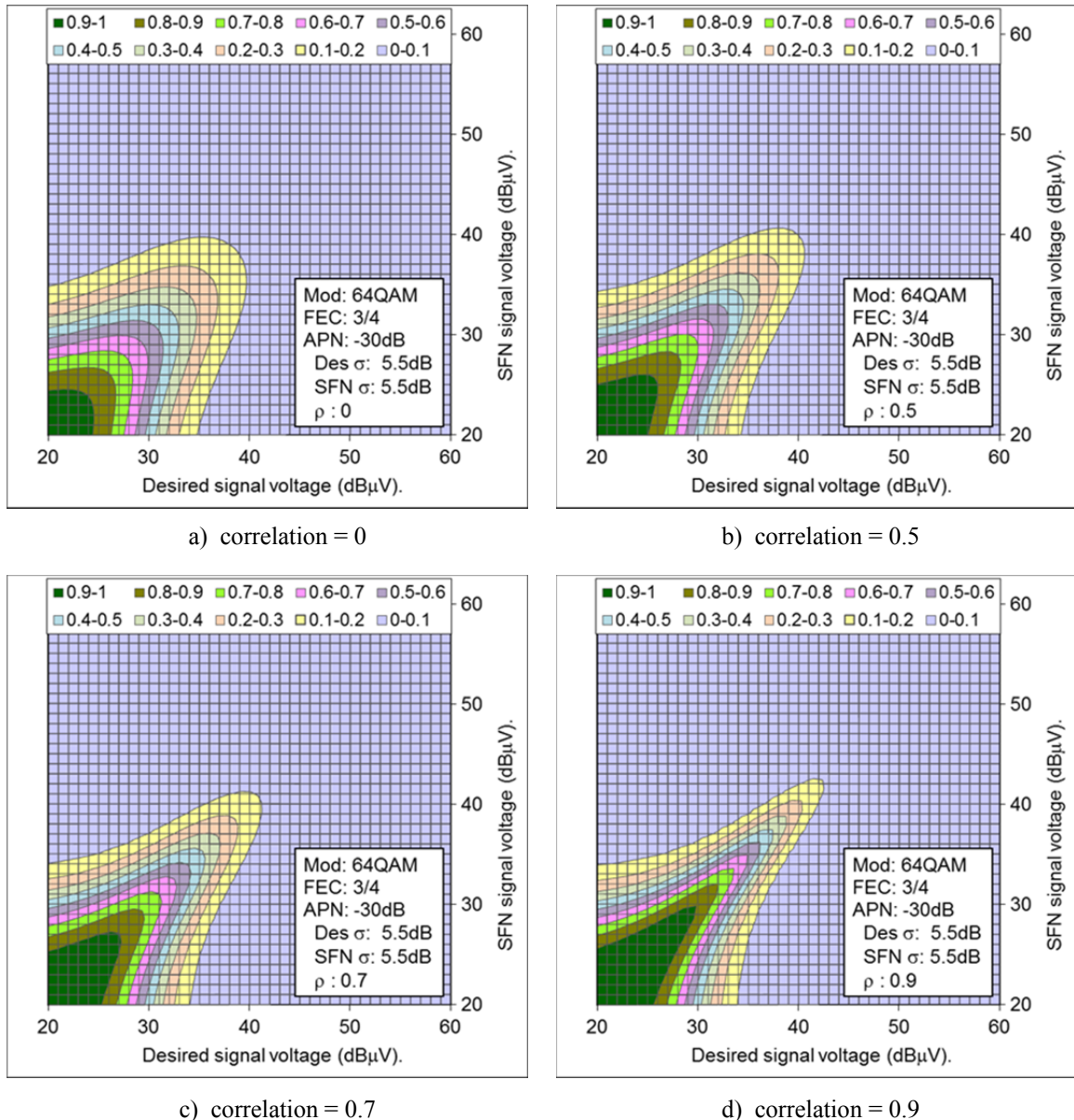
2 In the case of multiple SFN waves

In the case of a single SFN wave, the increases of required CNR can be uniquely defined by equation (7), because the frequency ripples at a receiver input are decided by sole parameter of the amplitude of SFN wave, i.e. U_a in equation (6). It cannot be unique in the case of multiple SFN waves, because the ripples take various forms depending on the amplitude, delay and phase of each SFN wave.

Figure 9 shows examples of frequency ripples generated by three waves (a main and two SFNs) at a receiver input. The total power of SFN waves is set at 0 dB (same as main wave) in both examples, but each SFN wave has a different amplitude as indicated in the figures. The increases of required CNR for 64-QAM-FEC7/8 are calculated to be 3 dB and 14 dB for Figs 9a and 9b respectively. Thus we cannot find a unique relationship between the total power of SFN waves and the increase of required CNR, and hence we will apply the statistical approach to analyse multiple SFN waves.

FIGURE 9

**Examples of frequency ripples**
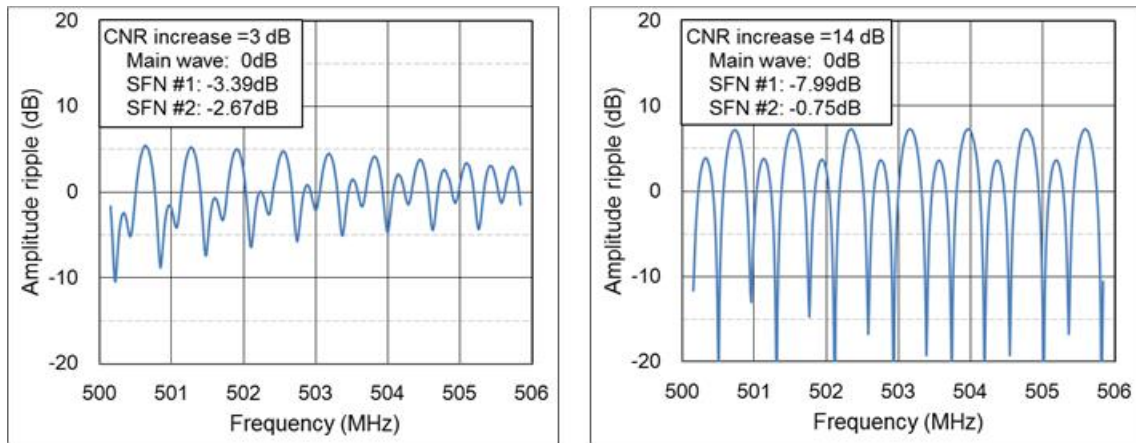
a) Little increase in required CNR

b) Large increase in required CNR

Figure 10 shows examples of the increase in required CNR, where each dot (orange coloured) represents the increase against a set of SFN waves having random amplitudes, delays and phases. Each graph contains 50 000 random trials. Figure 10a is for the case of 2 SFN waves, Fig. 10b for 3 SFN waves and Fig. 10c for 10 SFN waves. Since the strongest wave in the received signal is treated as the main wave, the dots do not exist in the range beyond the number of SFN waves (3 dB for 2 SFN waves, 4.8 dB for 3 SFN waves and so on). The maximum value in the horizontal axis takes place only when all received waves have an identical amplitude.

FIGURE 10

Examples of increase in required CNR (64-QAM-FEC7/8)
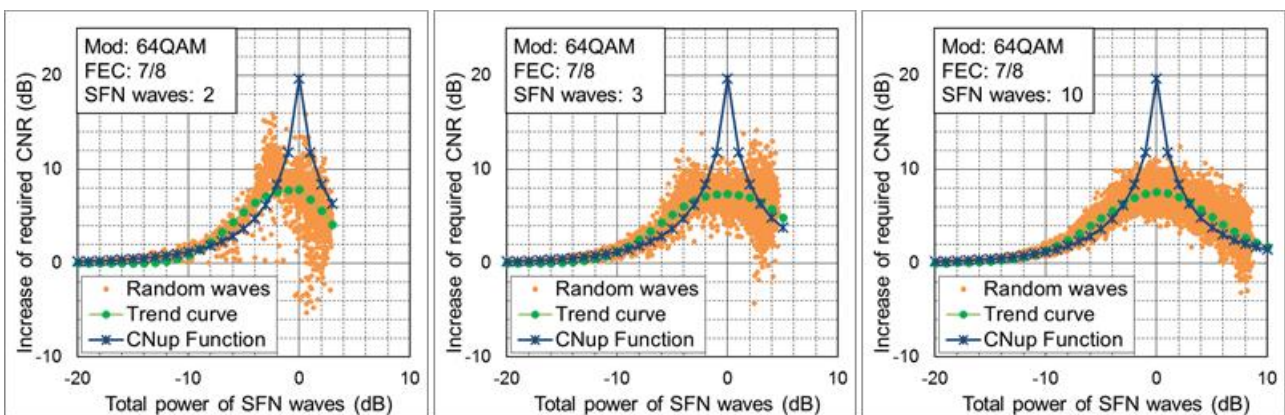

a) 2 SFN waves

b) 3 SFN waves

c) 10 SFN waves

2.1   Appropriate function to express multiple SFN waves

The green coloured curves in Fig. 10 express the trend curves for the increases of required CNR calculated against a number of random trials, and they are reproduced in Fig. 11a to show differences by the number of SFN waves. Figure 11b shows distribution of the increase in required CNR, where the horizontal axis denotes dB difference between the actual increase for random SFN waves and the trend curve. The vertical axis denotes cumulative percentage. The distributions are almost identical except for single SFN wave and we will adopt here the trend curve for 10 SFN waves as the representative one. It is seen from the figure that 90% of random trials are covered at a dB difference of 1.1 dB, 95% at 1.7 dB and 99% at 3.0 dB.

FIGURE 11

Trend curve and distribution of increase in required CNR (64-QAM)
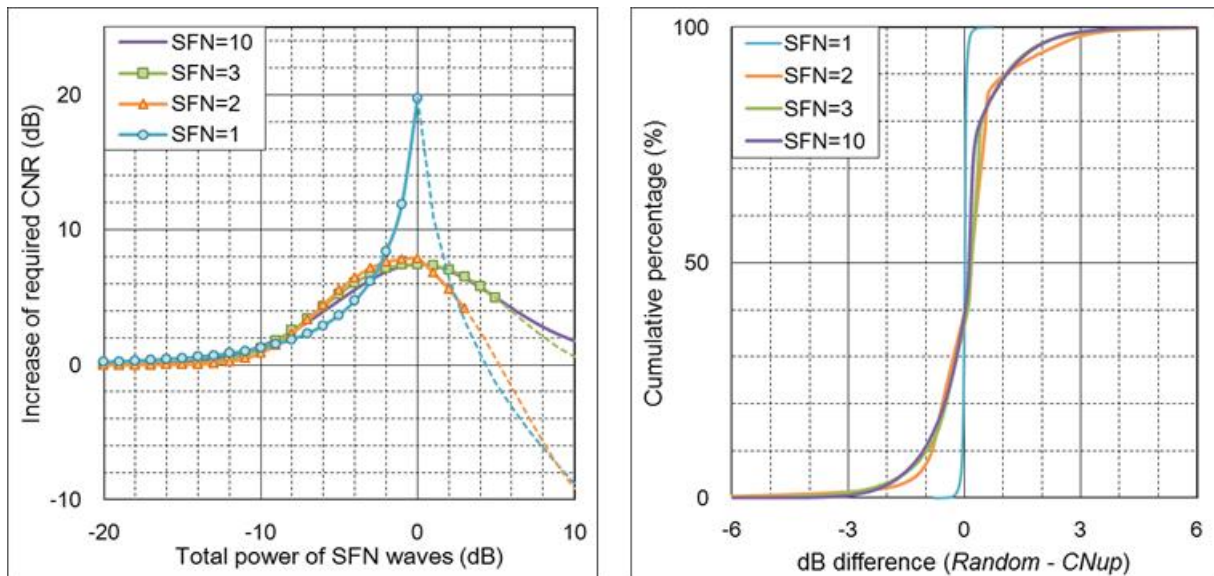
a) Trend curves (64-QAM)   b) Distribution of increases in required CNR (64-QAM-FEC7/8)

Trend curves are often used to express typical characteristics in the statistical sense. However, the trend curves shown in Fig. 11a have problem that they exhibit a large discrepancy between single SFN wave and multiple waves, and we have to select the appropriate one according to the number of SFN waves. Such selection is impractical, because the number of SFN waves are unknown in most cases or it may change by introduction of new TX stations/gap-fillers and by variations in propagation condition such as fading.

To avoid the above problem, we will adopt CNR Increase Functions shown in Fig. 12a as the appropriate functions that are to represent the increases of required CNR for multiple SFN waves. These functions are defined independent of the number of SFN waves. They apply the same coefficient values as equation (7) for α, β and γ. The values for coefficient A are obtained by least square approximation against a number of random trials, and are listed in Table 2 in § 1.3.

Figure 12b shows the distribution of difference (referred to "Difference Distribution" hereinafter) between actual increases of required CNR and CNR Increase Function. The graphs are similar to those for the trend curves, and 90% of random trials are covered at a dB difference of 1.6 dB, 95% at 2.3 dB and 99% at 3.7 dB. These values in dB difference are regarded as the margins that are added to CNR Increase Function to cover the designated percentage of random trials. Table 3 summarizes the margins for CNR Increase Function to cover 95% of random trials.

FIGURE 12

Appropriate function and increase of required CNR
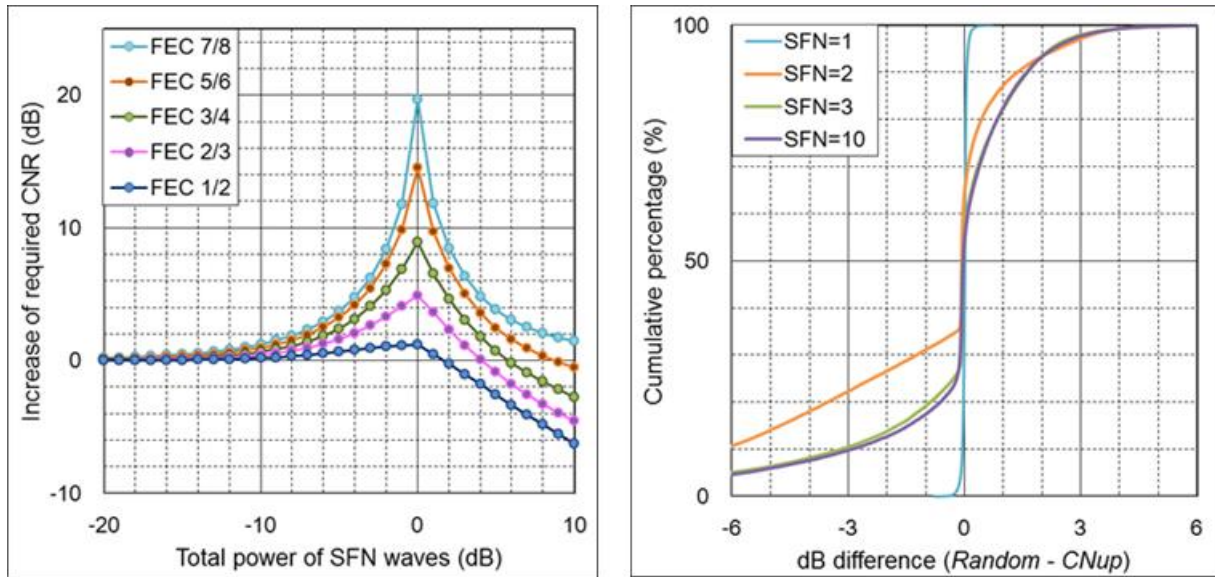
a) CNR Increase Function (64-QAM)   b) Distribution of increase in required CNR (64-QAM-FEC7/8)

TABLE 3

**Margins for CNR Increase Function to cover 95% of random trials**

	FEC 7/8	**FEC 5/6**	**FEC 3/4**	**FEC 2/3**	**FEC 1/2**
64-QAM	2.3 dB	1.3 dB	0.6 dB	0.4 dB	0.3 dB
16-QAM	2.8 dB	1.5 dB	0.7 dB	0.5 dB	0.3 dB
QPSK	3.6 dB	2.0 dB	1.0 dB	0.5 dB	0.3 dB

2.2   SFN failure probability in the case of multiple SFN waves

Probability of SFN failure caused by multiple SFN waves can be calculated based on equation (14). In the case of a single SFN wave, the integral boundary in equation (14) is uniquely determined by resolving equation (11). In the case of multiple SFN waves, the increases of required CNR distribute around CNR Increase Function, and consequently the integral boundary distributes, as shown in Fig. 13a.

FIGURE 13

Distributed integral boundaries and equivalent blurred signal points

a) Distributed integral boundaries

b) Equivalent blurred signal points
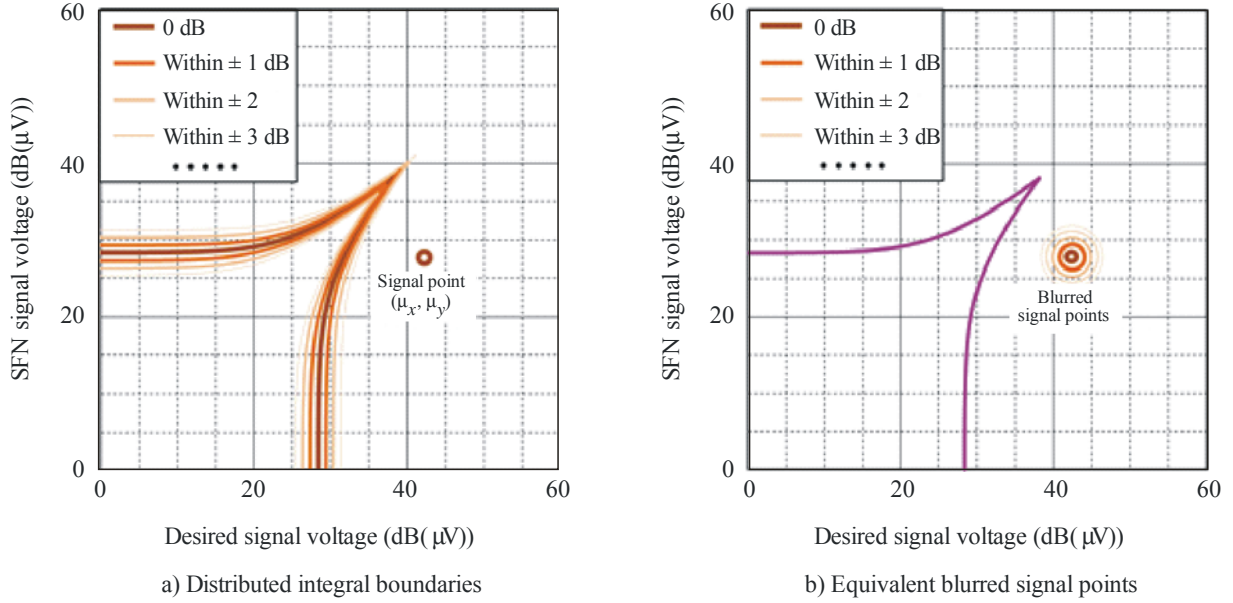
Report BT.2209-13

The integral calculation against the distributed boundaries in equation (14) is obtained by summing up the product of the definite integral against one of the distributed boundaries and the probability that the boundary takes place. Then we will obtain equation (15).

$$P(\mu_x, \mu_y) = \int \left[Prb(z) \times \underset{\text{SFN failure conditions}}{\iint} F(E_x, E_y) dE_x \, dE_y \right] dz \qquad (15)$$

where:

$Prb(z)$: probability density function of Difference Distribution

z : deviation from CNR Increase Function (or dB difference in Fig. 12b).

Equation (15) is impractical to calculate, and we will make approximation of it. Taking into account that $F(E_x, E_y)$ in equation (15) is a 2-dimensional normal distribution around a signal point at (μ_x, μ_y), we will assume here that the definite integral in the equation takes an identical value under either condition of a fixed boundary and blurred signal points (Fig. 13b) or the original condition of distributed boundaries and a fixed signal point (Fig. 13a). Further assuming that Difference Distribution is a normal distribution, we can use equation (14) with modified standard deviations instead of σ_x and σ_y in equation (13).

Since the distribution of field strengths (or signal voltages) and Difference Distribution are mutually independent events, the modified standard deviation is simply obtained by equation (16)

$$\sigma_{xm} = \sqrt{\sigma_x^2 + \sigma_{inc}^2} \quad \text{and} \quad \sigma_{ym} = \sqrt{\sigma_y^2 + \sigma_{inc}^2} \qquad (16)$$

where:

σ_{xm} and σ_{ym} : denote modified one for σ_x and σ_y

σ_{inc} : denotes standard deviation of Difference Distribution.

With the approximated calculation above, two independent distributions, expressed by σ_x (or σ_y) and σ_{inc}, are combined into a single distribution of σ_{xm} (or σ_{ym}). The values of σ_{inc} are obtained by dividing the margins listed in Table 3 by a factor of 1.64, as the margins are given for cumulative percentage of 95% which corresponds to 1.64 times the standard deviation.

When applying the field strength distribution of $\sigma_x = 5.5$ dB, the modified standard deviations are, for example, 6.0 dB for 64QAM-FEC7/8 and 5.53 dB for 64-QAM-FEC3/4, almost negligible changes to the original value of 5.5 dB. Thus the number of SFN waves gives little effects on SFN failure probability, and the considerations given in §§ 1.5-1.8 are generally applicable regardless of the number of SFN waves.

Chapter II

SFN with delays exceeding guard interval duration

When the delay of SFN wave exceeds the guard interval duration, the orthogonal features among OFDM carriers are lost, resulting in a large increase in the required DUR. The Japanese channel plan applies DUR = 28 dB including margins for several factors. It may be reasonable for the basic channel plan to include margins, because the basic plan should guarantee stable networks operation. If there were enough room in the spectrum, we could apply the plan values for each of the transmission stations. But there is not enough spectrum in the real world, hence we have to establish the appropriate values, which are required especially for small-scale transmission stations.

3   In the case of SFNs with delays exceeding guard interval duration

First we will analyse the characteristics of OFDM signals under the existence of SFN waves having delays exceeding guard interval duration. Then we will discuss about the receiver characteristics to be specified. We call the SFN with delays exceeding guard interval duration as "outer-GI SFN" in short.

3.1   SFN wave with a large delay exceeding guard interval duration

Since SFN signal with a very large delay has no correlation to the desired signal, we can treat it as random noise. The required DUR is calculated by the following equation:

$$CN_0 = \frac{C_{rms}^2}{N_{fix}^2 + U_{rms}^2} \quad \text{and} \quad DU_0 = \frac{C_{rms}^2}{U_{rms}^2}$$

$$\therefore \quad DU_0 = \frac{CN_0}{1 - CN_0 \cdot \left(N_{fix}^2 \big/ C_{rms}^2\right)} \tag{17}$$

where:

C_{rms} and U_{rms}:   denote *r.m.s.* amplitude of the desired wave and of the SFN wave respectively

N_{fix}:   denotes fixed noise of receiver

CN_0:   ratio of desired signal to unnecessary components (the same values as the reference CNR)

DU_0:   required DUR.

3.2 SFN with relatively small delays (but larger than guard interval duration)

We will analyse the demodulated signals when an outer-GI SFN wave exists. We assume the amplitude of delayed signal to be U and the portion of the delay exceeding GI to be τ (normalized by FFT interval).

In Fig. 14, the demodulated signals are obtained by multiplying each of OFDM carriers to the input signal and then integrating each product over the FFT interval. Assuming the original OFDM signal to be expressed by equation (18), then the demodulated component for the main signal (X) and that for delayed signal (Y) are written as below:

$$S_o = \sum A_k \exp(j2\pi kt) \tag{18}$$

$$X = \int_0^1 \sum A_k \exp(j2\pi kt) \times \exp(-j2\pi k_o t)\,\mathrm{d}t = \int_0^1 \sum A_k \exp(j2\pi(k-k_o)t)\,\mathrm{d}t = A_{ko} \tag{19}$$

$$Y = U\left[\int_0^\tau \sum B_k \exp(j2\pi kt) \times \exp(-j2\pi k_o t)\,\mathrm{d}t + \int_\tau^1 \sum A_k \exp(j2\pi kt) \times \exp(-j2\pi k_o t)\,\mathrm{d}t\right] \tag{20}$$

FIGURE 14

OFDM demodulation
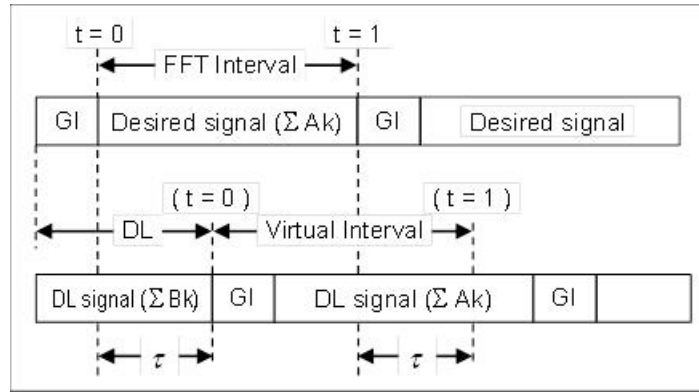
Taking into account the guard interval, the integral of the 2nd term in equation (20) has the same result as integrating over "virtual interval" instead of "FFT interval" shown in Fig. 14.

$$\begin{aligned} 2nd\ term &= U\left[\int_0^1 \sum A_k \exp(j2\pi(k-k_o)t)\,\mathrm{d}t - \int_{1-\tau}^1 \sum A_k \exp(j2\pi(k-k_o)t)\,\mathrm{d}t\right] \\ &= UA_{ko} - U\int_{-\tau}^0 \sum A_k \exp(j2\pi(k-k_o)t)\,\mathrm{d}t \end{aligned} \tag{21}$$

$$Y = UA_{ko} + U\int_0^\tau \sum B_k \exp(j2\pi(k-k_o)t)\,\mathrm{d}t - U\int_{-\tau}^0 \sum A_k \exp(j2\pi(k-k_o)t)\,\mathrm{d}t \tag{22}$$

The 1st term in equation (22) represents the signal component, the 2nd term inter-symbol interference, and the 3rd term inter-carrier interference. Thus, the delayed signal, of which delay exceeds the guard interval, includes the signal component, and we call it as "effective inner-GI component". This component interferes with the main signal and produces ripples in frequency response, resulting in the required CNR increase. This can be treated in the same way as the inner-GI SFN wave with an exception of interfering duration, which is $(1 - \tau)$ instead of FFT interval.

The inter-symbol interference, i.e. the 2nd term in equation (22) has no correlation with the signal

component; it can be treated as random noise of which power increases in proportion to τ.

The expectation of 3rd term increases in proportion to τ when τ is close to zero, although the value itself varies according to the signal components A_k. Since the 3rd term equals to signal component when $\tau = 1$, the expectation of interference component is in proportion to $(1 - \tau)$ when τ is close to 1. Thus, the inter-carrier interference, i.e. the 3rd term in equation (22) can be regarded as random noise of which power increases in proportion to $\tau(1 - \tau)$. We call these components that have no correlation to the signal as "effective outer-GI component", and we can treat them in the same way as random noise.

Taking into account the above features of the 2nd and 3rd terms in equation (22), we can obtain the required DUR under outer-GI SFN environments by resolving equation (23).

$$Required\,CNR = CN_0 + CN_{up}\big(U\mathrm{dB} + 10\cdot\log\left(1 - \tau\right)\big) \qquad \mathrm{dB}$$

$$Noise\,Component = \tau U_{rms}^2 + \tau(1 - \tau)U_{rms}^2 + N_{amp}^2 \qquad (\text{in real number expression})$$

$$-10\cdot\log\big(\tau U_{rms}^2 + \tau(1 - \tau)U_{rms}^2 + N_{amp}^2\big) = CN_0 + CN_{up}\big(U\mathrm{dB} + 10\cdot\log(1 - \tau)\big) \qquad (23)$$

where:

$\quad U_{rms}^2$:   denotes power of delayed wave

$\quad N_{amp}^2$:   noise power of APN

$\quad CN_0$:   reference CNR (dB)

$\quad CN_{up}(*)$:   CNR Increase Function (dB)

$\quad U\mathrm{dB}$:   power of delayed wave (dB).

The solution of equation (23) at $\tau = 0$ corresponds to the required DUR for inner-GI SFN environment. When the equation has no solution at $\tau = 0$, the SFN failure does not takes place.

Equation (24) is a concrete example of equation (23), and Fig. 15 shows the corresponding graphs for the equation. Figure 16 shows the relationship between delay and required DUR, which is called "bathtub curve".

$$Required\ CNR = CN_0 + \alpha\cdot\exp\big(-\big|\beta\cdot(U\mathrm{dB} + 10\cdot\log(1 - \tau))\big|^{\gamma}\big)$$
$$Noise\ Component = \big(2\tau - \tau^2\big)10^{U\mathrm{dB}/10} + 10^{Namp\mathrm{dB}/10} \qquad (24)$$

where, α, β and γ are shown in Table 2 in § 1.3.

FIGURE 15

Required CNR and interference component under outer-GI environment
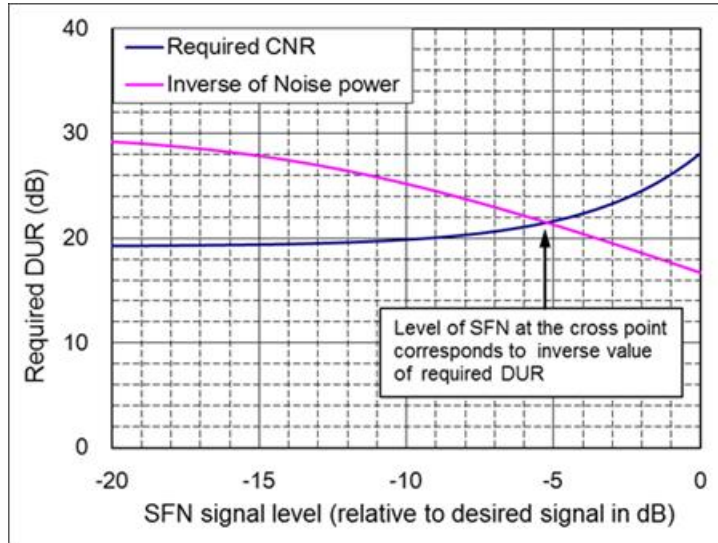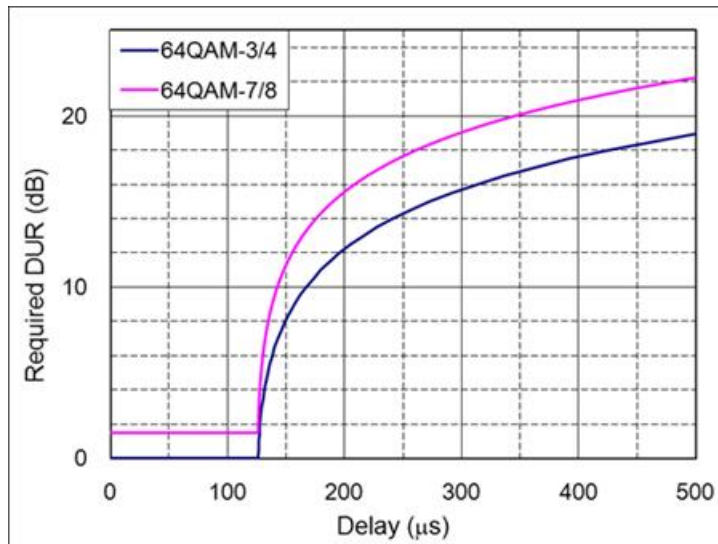

FIGURE 16

Bathtub curve (calculated for APN of –35 dB)

3.3   Aliasing effects of scattered pilot signals

In the previous section, we have analysed the interference components in the OFDM demodulation process, in which we assumed implicitly that the rippled frequency response was ideally compensated by some means. This compensation process is equivalent to regenerate each of OFDM reference carriers from the received scattered pilot signals (SP hereinafter). As the SP signals are sent in every 3 OFDM carriers, the minimum frequency spacing in the ripples measured with the SP signals is limited, that is, the maximum delay that can be observed is limited. If there is a delayed wave exceeding this maximum value, correct observation cannot be performed, just as aliasing found in general sampling process.

Figure 17 explains the above circumstance of SP signal. The figure shows the frequency response when delayed waves with a long delay and a short delay coexist. The frequency response has fine ripples due to the long delay wave, and the OFDM carriers take the values as shown by * marks in the figure. On the other hand, we will estimate the ripples to be a rough curve as shown in the

figure, because we can observe the response sampled only at the SP signals. Therefore, the carrier references to be used in the demodulation include errors in phase and amplitude.

FIGURE 17

Frequency response estimated from SP signals
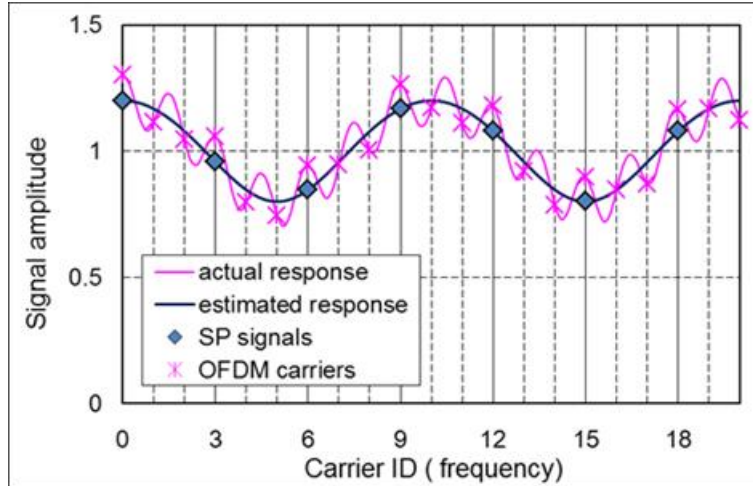
The average error can be estimated in the same way as the general analysis of distortions included in the signal recovered from the sampled values, although the error of each carrier varies depending on the delay and amplitude of SFN waves, characteristics of the interpolation filter, and so on.

The average error (A_e^2) can be written as follows:

$$A_e^2 = \sum outband\ \ components + \sum interpolation\ \ error\ \ components \qquad (25)$$

Note that in analysing a sampling system, the usual way is that the original function is a time-domain function and the conversion function is the Fourier spectrum, while in equation (25), the original function is Fourier spectrum and the conversion function is the time-domain one.

Figure 18 shows the out-band components and interpolation errors used in equation (25). The figure is the case for the FFT interval of 1 008 μs, and the value 336 μs corresponds to 1/3 of the FFT interval.

FIGURE 18

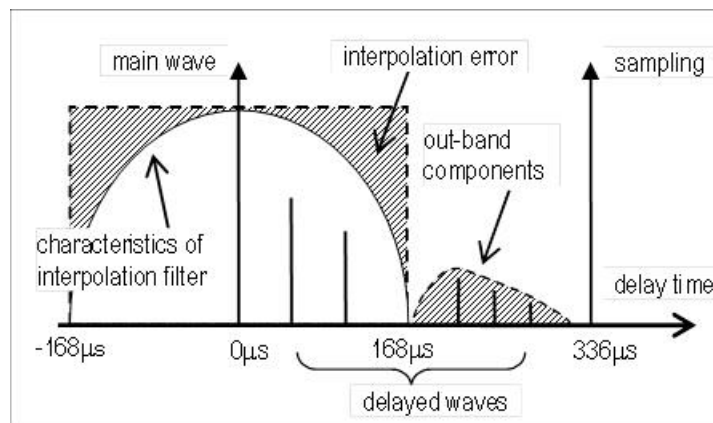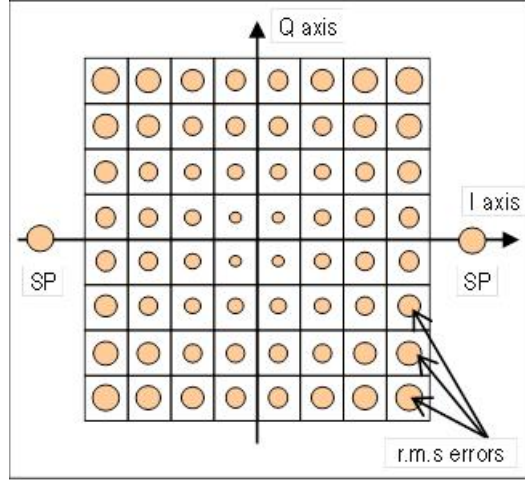**Delay profile, out-band components and interpolation errors**

FIGURE 19

Effects of carrier recovery errors

The effects of carrier recovery errors differs by signal points on the constellation, as shown in Fig. 19. It is large on the signal points at outer side of the constellation. To simplify the calculation, we assume here that the *r.m.s.* error at every signal point has the same error at the SP point. This simplification results that the calculated BER tends to become worse than that of actual one.

3.4 Calculation method for required DUR

When there are many kinds of interference factors, the required DUR can be written in general form as below:

$$\frac{1}{CN_0} = W_1\left(U^2\right) + W_2\left(U^2\right) + \bullet\bullet\bullet$$

$$Required\ DUR = -10\log\left(U^2\right) \qquad \text{dB}$$

(26)

where:

CN_0:　denotes the required CNR that is determined by modulation and FEC (such as 19.2 dB for 64-QAM-FEC3/4)

U^2:　denotes the power of delayed signal

$W_1(*)$, $W_2(*)$, etc.:　represent the weighting functions which convert the delayed signal into the equivalent noise power against each interference factor.

The major factors that affect correct reception are inter-symbol interference (2nd term in equation (22)), inter-carrier interference (3rd term), and carrier recovery error which we are discussing in this section.

Referring to equation (23), we apply equation (26) as below:

$$\left[CN_0 \cdot CN_{up}\left(U_{rms}^2\right)\right]^{-1} = N_{amp}^2 + \tau \cdot U_{rms}^2 + \tau\left(1-\tau\right)\cdot U_{rms}^2 + \left(1-\tau\right)\cdot A_e^2$$

(27)

The 2nd, 3rd and 4th terms in the right side of equation (27) correspond to inter-symbol interference, inter-carrier interference, and carrier recovery errors, respectively. Note that we neglect the fixed noise assuming the received signal to be enough high. Resolving equation (27) for U^2, the required DUR is obtained by the inverse number of U^2.

The hardware characteristics that affect the receiver performance are N_{amp}^2 and A_e^2 in equation (27), and the other terms are independent of hardware characteristics. Therefore, we have to specify these two for the reference receiver to be applied in network design.

The actual values of amplitude proportional noise were at –35 dB for the worst receivers available on the market. So we have adopted this –35 dB as the specification of APN.

Before we specify the interpolation filter characteristics, we will take an overview on the filter characteristics. When assuming an ideal LPF as the interpolation filter, equation (27) is written as below:

$$\left[CN_0 \cdot CN_{up}\left(U_{rms}^2\right)\right]^{-1} = N_{amp}^2 + \tau U_{rms}^2 + \tau(1-\tau)U_{rms}^2 \qquad (|\text{delay}| < 168\mu s)$$

$$\left[CN_0 \cdot CN_{up}\left(U_{rms}^2\right)\right]^{-1} = N_{amp}^2 + \tau U_{rms}^2 + \tau(1-\tau)U_{rms}^2 + (1-\tau)U_{rms}^2 \qquad (|\text{delay}| \geq 168\mu s)$$

(28)

In this case, the OFDM carriers can be recovered perfectly and no recovery errors take place when the delay is within the Nyquist band. When the delay is out of Nyquist band, A_e^2 equals to the power of the delayed wave itself.

In the case where the interpolation filter is not an ideal LPF, the power of interpolation errors (A_e^2) is calculated by the below:

$$A_e^2 = \sum_{|DL_j| < 168\mu s} \left[\left(1 - LPF(DL_j)\right) \cdot U_j\right]^2 + \sum_{|DL_k| \geq 168\mu s} U_k^2$$
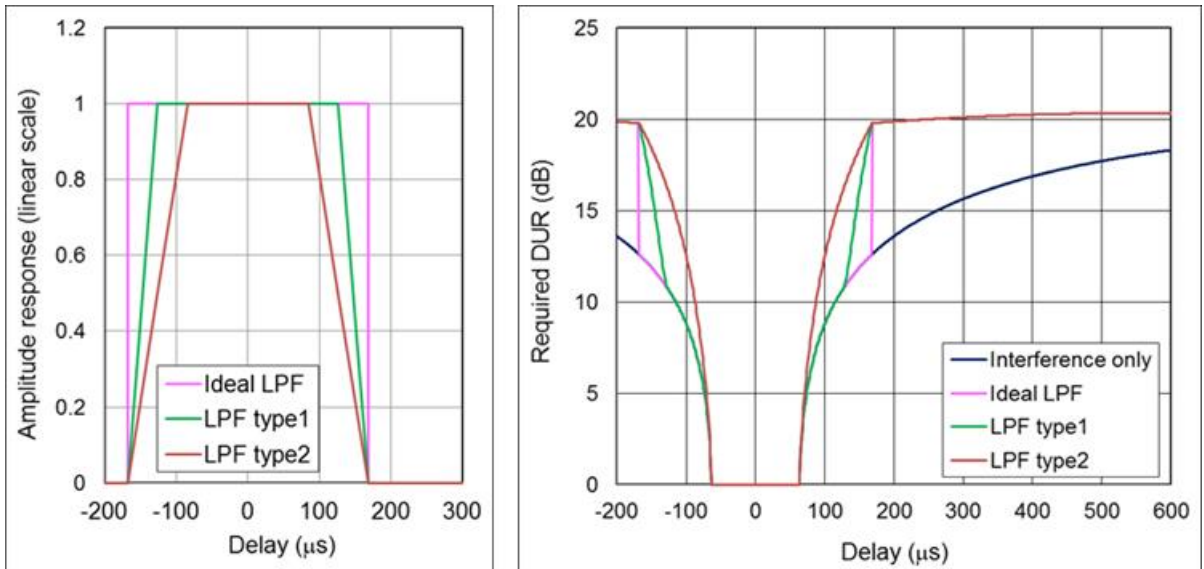
(29)

where:

        U_j: represents the amplitude of delayed waves within the Nyquist band ($|DL| < 168\mu s$)

        U_k: amplitude of delayed waves outside the Nyquist band ($|DL| \geq 168\mu s$).

Figure 20 shows examples of calculation results for some interpolation filters.

FIGURE 20

Interpolation filter and corresponding DUR characteristics (by equation (29))

3.4.1 Re-consideration on aliasing effects of scattered pilot signals

We have assumed the aliasing effects of SP signals to be in proportion to the average error power A_e^2. However, the required DUR of actual receivers is higher by 1 dB than that calculated by equation (27). This suggests that the carrier recovery errors are affected by other factors in addition to the average error power.

The recovery error for each OFDM carrier corresponds to the error voltage of that carrier but not to the *r.m.s.* error voltage. The error voltage differs from carrier to carrier, and hence the BER differs carrier by carrier. In these cases where the error voltage differs by carrier, the total BER averaged over all carriers becomes worse compared to the case where every carrier takes the same error voltage. This is because the BER degradation of the carriers with error voltages larger than the average is more severe compared to the BER improvement of the carriers with smaller error voltages. Therefore, we need to add a new term in equation (27) to express the effects due to error voltages being different from carrier to carrier.

However, it is quite difficult to derive theoretically such effects. Considering that the effects may differ depending on the delay and/or phase of the input waves, and that the amount of effect is only 1-2 dB, we introduce a new coefficient to be consistent with the measured results, as below:
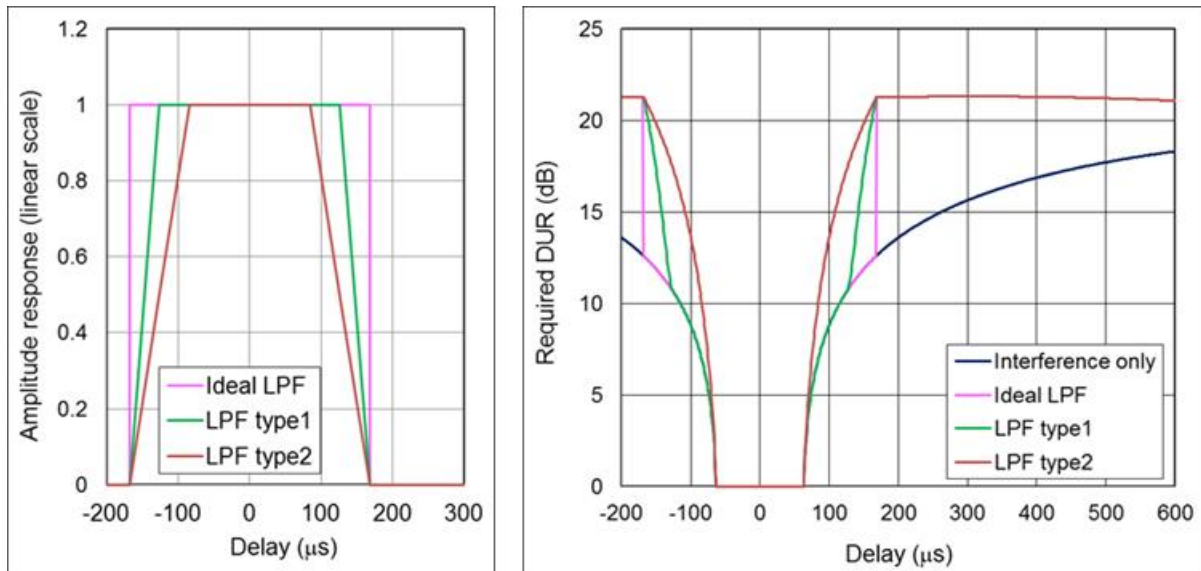
$$\left[CN_0 \cdot CN_{up}\left(U_{rms}^2\right) \right]^{-1} = N_{amp}^2 + \tau \cdot U_{rms}^2 + \tau\left(1-\tau\right) \cdot U_{rms}^2 + 1.5 \cdot \left(1-\tau\right) \cdot A_e^2 \qquad (30)$$

here, the value for the new coefficient to be 1.5.

Figure 21 shows the examples calculated by equation (30).

FIGURE 21

Interpolation filter and corresponding DUR characteristics (by equation (30))


3.5 Setting of FFT window

Figure 22 shows the relationship between the FFT window in a receiver and the required DUR characteristics or the bathtub curve. The figure is the case of guard interval of 126 µs (1/8 of FFT frame duration).

Figure 22a shows the bathtub curve due only to the interference components, i.e. inter-symbol interference and inter-carrier interference. Figure 22b represents the characteristics of interpolation

filter, which has a unity response within the bandwidth of ±LPFbw and zero response outside the Nyquist band (±168 μs). Figure 22c shows the overall bathtub curve, which includes all the factors.

A receiver adjusts its FFT window in such a way that the main wave is positioned at the bottom of the bathtub curve. Otherwise, a large inter-symbol interference takes place. Therefore, the adjustment range of the FFT window is limited within $\pm GI/2$ (GI denotes guard interval duration). In the actual hardware, some margins are necessary to avoid miss-adjustment, and the adjustment range of FFT window is limited within $\pm(GI/2 - T_m)$ as shown in the figure. Note that the position of "0 μs" in Fig. 22c is different from Figs 22a and 22b, as it is a custom to express the delays relative to the main wave.

FIGURE 22

FFT window and bathtub curve
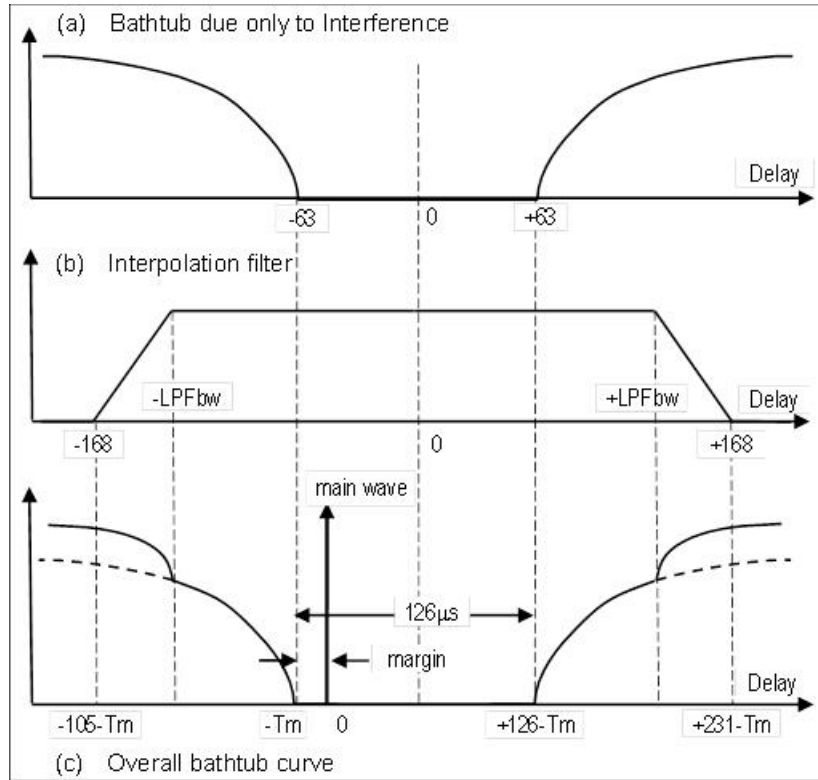
3.5.1 Optimum position of FFT window

Here we summarize how to estimate the reception failure.

1) To split each SFN wave into effective inner-GI component and effective outer-GI component.

    Regarding effective inner-GI component, we assume one equivalent SFN wave of which power is equal to the sum of each effective inner-GI component, that is,

$$U_{eq}^2 = \sum_k (1 - \tau_k) U_k^2 \tag{31}$$

    Regarding effective outer-GI component, we assume equivalent noise, which is the sum of inter-symbol interference; inter-carrier interference and carrier recovery error of each SFN wave, that is,

$$N_{eq}^2 = \sum_k \tau_k U_k^2 + \sum_k \tau_k (1 - \tau_k) U_k^2 + 1.5 \cdot \sum_k (1 - \tau_k)(1 - LPF(DL_k))^2 U_k^2 \tag{32}$$

2) To sum up all of the non-correlated noise powers, which are fixed noise, co-channel digital waves (with different programs) and co-channel analogue waves in addition to equation (32), that is,

$$N_{total}^2 = N_{fix}^2 + N_{eq}^2 + \sum_k CoD_k^2 + \sum_k CoA_k^2 / AtoD^2 \qquad (33)$$

where, N_{fix}^2 denotes the fixed noise, CoD_k^2 the power of a co-channel digital wave with different programs, CoA_k^2 the power of a co-channel analogue wave, and $AtoD^2$ the weighting factor with which the analogue signal is dealt as equivalent random noise.

3) To calculate the probability of failure occurrence, using equations (11) and (14), in which the total noise power is given by equation (33). In this case, the optimum position of the FFT window is defined to be such one that minimizes the value of equation (33).

4) To apply the following methods described in paragraphs 5) and 6) instead of the above paragraph 3), as it is not practical to calculate equation (11).

5) To plot the signal voltages of the desired wave and the equivalent inner-GI SFN wave on the 2-dimensional voltage diagram, as shown in Fig. 23 (green coloured mark). To shift this input point to the point shown by brown coloured mark (left down direction). The value of sift is given by the following equation:

$$10 \log\left(N_{total}^2 / N_{fix}^2\right) \quad \text{dB} \qquad (34)$$

6) To apply equation (14) against the equivalent input voltage, i.e. the shifted point in the figure.

FIGURE 23

Equivalent input signal voltages

Report BT.2209-23
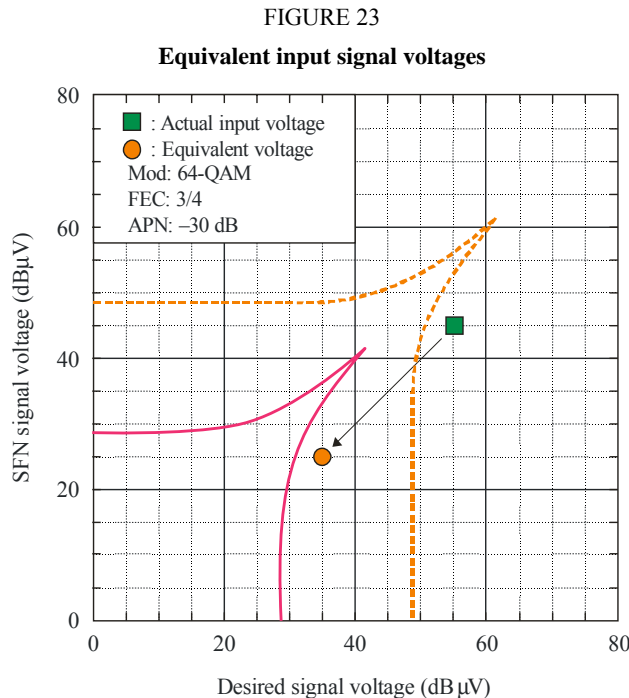
The optimum position of FFT window is stated in the above § 3, but it is not useful to apply equation (33) from the view point of computation hours. Therefore we introduce the following alternative method.

Figure 24 shows the relationship between the input waves and FFT window position. The curve named "GI Mask characteristics" in the figure is the inverse bathtub curve (opposite polarity in dB), which indicates the maximum allowable levels of delayed signals. The receiver adjusts its FFT window so that all delayed waves become below the mask. If a delayed signal exceeds the mask, the receiver cannot receive the signal correctly.

When there are many delayed signals of which amplitudes are close to (still below) the mask, the receiver may fail correct reception. So, we introduce a new concept of "faulty power", which is defined to be the difference in dB between the amplitude of delayed signal and the corresponding mask. When the sum of the faulty power is larger than 0 dB, we regard the delayed signals to exceed the mask as a whole. We also assume that the receiver adjusts its FFT window to minimize the total faulty power, as written in the following equations:

$$PdB_k = UdB_k^2 - MaskdB(DL_k) \qquad \text{(dB)}$$
$$P_{und} = \sum_k 10^{PdB_k/10} \rightarrow \text{minimize} \tag{35}$$

FIGURE 24

Optimum setting of FFT window
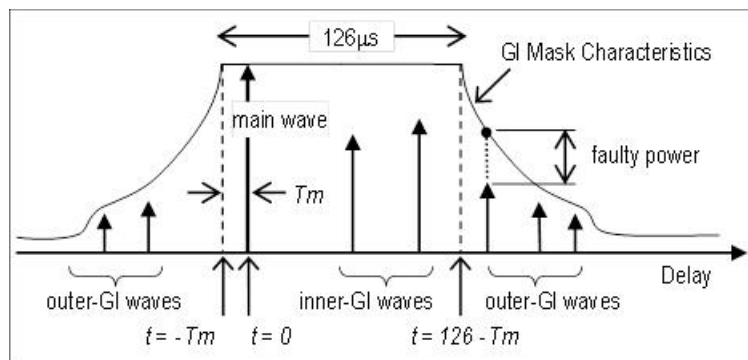
3.6 Protection ratios for analogue to digital interference

The effects of interference from analogue signal depends not only on the receiver characteristics but also on the analogue signal or analogue program contents. We consider here the protection ratio against the worst-case analogue signals.

We have tested several receivers on the protection ratios, in which we apply colour-bar with 100% modulated stereo signal as the worst-case analogue signal. The results measured for the worst receiver is as follows.

         for 64-QAM-FEC3/4   protection ratio of 5 dB

         for 64-QAM-FEC7/8   protection ratio of 13 dB.

3.7 Receiver characteristics to be specified

As discussed above, many of the factors related to SFN reception are caused by OFDM itself, and are automatically defined by the signal parameters applied. The factors caused by hardware, which should be specified for the reference receiver, are listed in Table 4 together with the ARIB specifications.

TABLE 4

Factors to be specified

Item	ARIB specification	Remarks
Amplitude proportional noise	−35 dB	Relative to input signal level
Interpolation filter for carrier recovery	Flat	−126 μs ~ 126 μs
	Transition	−168~ −126 μs and 126~168 μs
FFT window setting margin	6 μs	
Protection ratio interfered by analogue TV	5 dB	64-QAM-FEC3/4
	13 dB	64-QAM-FEC7/8

3.8　　　GI Mask characteristics of receivers on the market

Figure 25 shows examples of guard interval mask of receivers available on the market together with the characteristics (denoted by "ARIB" in the figure) specified in § 3.7. Receivers except for the one expressed by dot line in the figure exhibit better characteristics than the ARIB specification. The dot-lined receiver is one that was produced before the ARIB specification has been established. The characteristic difference among receivers comes from the characteristics of interpolation filter used for reference carrier recovery (see § 3.3).

FIGURE 25

GI Mask of receivers available on the market
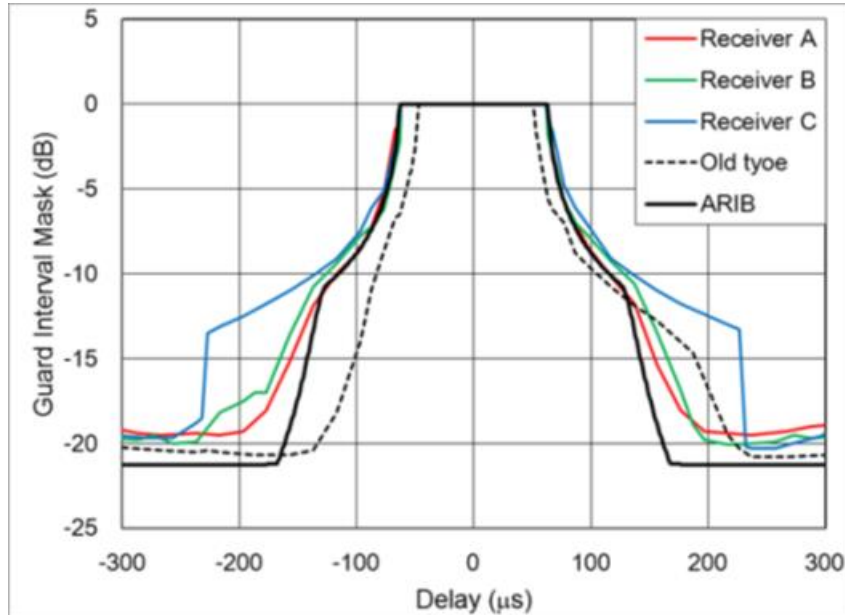
Chapter III

Adjacent channel interference

4 Major factors affecting on interference performance

The interference of adjacent channel and/or any other channels than the desired channel (referred to "out-channel" hereinafter) is caused by receiver itself. It is obvious that no interference would occur if an ideal BPF is inserted at the receiver input terminal. Major factors affecting the interference performance are intermodulation noise generated at the first stage amplifier, out-channel suppression characteristics of filters, clip and quantization noise of A/D converter and aliasing noise in digital processes.

We will consider the inter-relationships of the factors and derive a simple equation to express the out-channel interference performance of a receiver.

4.1 Receiver configuration

Figure 26 shows the basic receiver configuration together with the major factors affecting the interference performance. Although there are many types of receivers that provide different configurations such as "silicon tuner", the factors to be considered are common. For example, direct conversion type receivers, which convert the RF signal directly into the baseband using quadrature detection, equipped with "LPF" instead of "IF Filter" to reduce undesired out-channel signals, where the factor to be considered is "out-channel suppression characteristics" but not the filter types. So are the other factors.

Image channel suppression characteristics are one of the factors to be considered with conventional type receivers, but will not be treated in this document. Recent digital receivers use double conversion or direct conversion scheme that provides superior suppression performance.

FIGURE 26

Equivalent configuration of a receiver
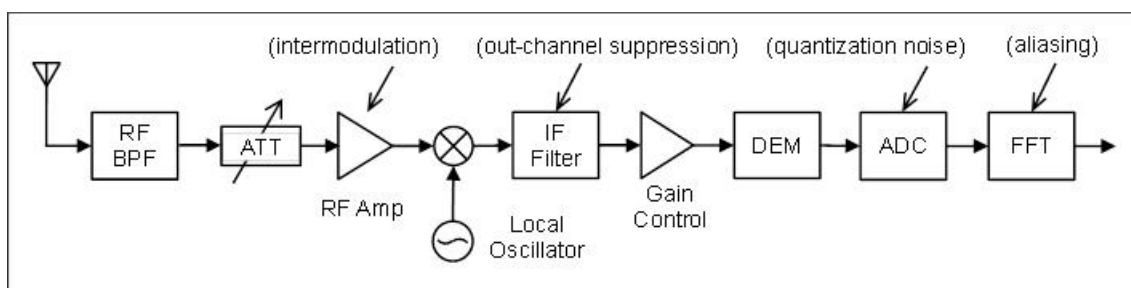
4.2 Unnecessary components

Unnecessary components in a receiver are fixed noise N_{fix} mainly generated in the first stage amplifier, intermodulation noise caused by non-linear characteristics of the amplifier, quantization noise of A/D converter and out-channel components being suppressed by IF filter.

Input-output characteristics of the first stage amplifier are generally approximated by a 3rd order polynomial, where the intermodulation noise is in proportion to the 3rd power of the input signal as below.

$$\textit{Intermodulation noise} \propto (D+U)^3$$

where:

D and U denote the power of desired signal and of out-channel signals, respectively.

The intermodulation noise depends not only on the amplifier's non-linear characteristics and signal levels but also on the signal spectra and frequency spacing between desired and undesired signals. For details, see Appendix 2.

The "Gain Control" circuit in the figure controls its output signal to remain within the dynamic range of A/D converter. When out-channel signals exist at large levels, the circuit must reduce its gain regardless of the desired signal level in order not to generate severe clipping noise, resulting in the desired signal being reduced. Consequently the quantization noise (and accompanied clipping noise) relative to desired signal is in proportion to the input signal to A/D converter as well as the APN value (e.g. $0.000316 = -35$ dB) as expressed below.

$$Quantization \ noise = APN \cdot \left(D + U/R \right)$$

where R denotes suppression ratio of IF filter for out-channel signals. The value of R may or may not change by out-channel frequencies.

By summing up these noises and out-channel components, the overall unnecessary component N_{eq} is written as below.

$$N_{eq} = N_{fix} + APN \cdot \left(D + U/R \right) + N_{im} \cdot \left(D + U \right)^3$$
$$N_{im} = X_{sat}^{-2} \big/ 50$$

(36)

where:

N_{im}:   denotes a coefficient expressing the degree of amplifier's non-linearity (see Appendix 2)

X_{sat}:   denotes input signal level at which the amplifier just saturate.

Figure 27a shows an example of unnecessary components calculated under the condition of APN of $0.000316 \ (= -35$ dB), out-channel suppression ratio of 100 ($= 20$ dB), amplifier saturation of 109 dBμV (0 dBm) and desired signal level of 60 dBμV (-49 dBm). The horizontal axis of the graph denotes out-channel signal level and the vertical axis unnecessary component, both relative to desired signal. The overall unnecessary component begins to increase at the out-channel signal level of 20 dB, which corresponds to out-channel suppression ratio of the IF filter. The intermodulation noise is lower than the quantization noise as for this condition.

4.3 Out-channel interference immunity

We define the allowable limit of out-channel signal to be the level that gives threshold CNR for desired signal. It is obtained by resolving the following equation for U.

$$CN_{threshold} = \frac{D}{N_{eq}} = \frac{D}{N_{fix} + APN \cdot \left(D + U/R \right) + N_{im} \cdot \left(D + U \right)^3}$$

(37)

Figure 27b shows the calculation results of equation (37) in the case of 64-QAM-FEC3/4. The dot line shows the case of ideal amplifier (without intermodulation noise) and the three curves correspond to SFN conditions, i.e. no SFN wave, SFN waves of -3 dB and 0 dB, for which threshold CNRs are increased according to the CNR Increase Function.

The allowable limit increases in proportion to the desired signal in the range lower than around 50 dBμV. In this range, the interference immunity or threshold undesired-to-desired ratio (UDR) takes constant values, such as 35 dB for no SFN wave, 31 dB for SFN of -3 dB and 24 dB for SFN

of 0 dB. This is because the overall unnecessary component increases in proportion to desired signals as shown in Fig. 27a.

FIGURE 27

Unnecessary components and out-channel interference characteristics
($APN = -35$ dB, $R = 20$ dB, $X_{sat} = 0$ dBm)
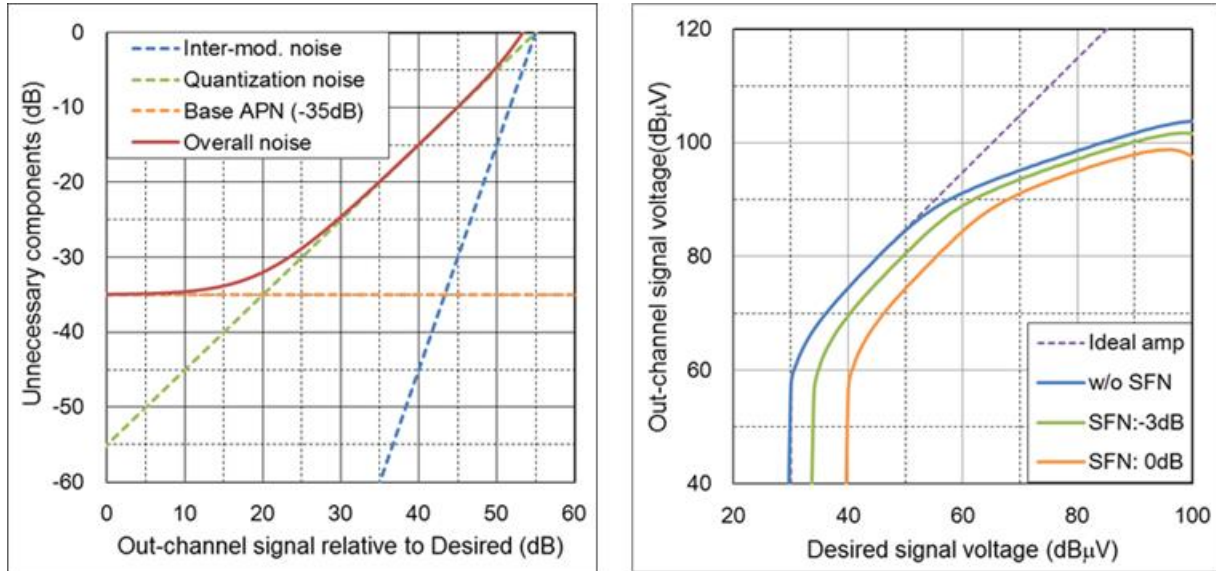
a) Unnecessary components   b) Out-channel interference characteristics

The allowable limit exhibits saturation for desired signals higher than around 60 dBµV where the intermodulation noise becomes dominant. In this range, the threshold UDRs decrease with desired signal being higher, such as 18 dB for no SFN wave, 17 dB for SFN of –3 dB and 15 dB for SFN of 0 dB at the desired signal of 80 dB(µV).

Figure 28 shows another example with a high out-channel suppression ratio of 50 dB. In this example, the out-channel signals are suppressed enough that the quantization noise has little effects on the interference characteristics. The threshold UDRs are high at low desired signals, such as 38 dB for no SFN wave, 37 dB for SFN of –3 dB and 35 dB for SFN of 0 dB at the desired signal of 50 dBµV, while they decrease with desired signal being higher.

The saturation in the allowable limits can be relaxed by inserting an attenuator at the receiver input (see Fig. 26) and by controlling it appropriately in accordance with input signal levels. In this case, the values of fixed noise N_{fix} and amplifier saturation level X_{sat} in equation (37) are replaced by those increased according to the attenuation, as follows.

$$N_{fix} \Rightarrow N_{fix} \cdot 10^{ATTdB/10} \quad and \quad X_{sat} \Rightarrow X_{sat} \cdot 10^{ATTdB/10}$$

where:

   *ATTdB*   denotes attenuation of the attenuator in dB.

Figure 29 shows examples when the attenuator is controlled. The saturation level shown in the figure depends on how to control the attenuator, but may be determined by other reasons than equation (37), such as protection of amplifier from breakdown. The examples apply the maximum input level to be 109 dBµV or 0 dBm.

As discussed above, the out-channel interference characteristics depend on the three major parameters, i.e. APN, out-channel suppression ratio R and amplifier's 3rd order distortion coefficient N_{im}. The characteristics are given on a 2-dimensional diagram of desired and out-channel signals

by resolving equation (37). It is insufficient to express the characteristics by a single figure of adjacent channel rejection ratio (sometimes referred to adjacent channel protection ratio). It should be noted that the out-channel interference characteristics depend on SFN conditions.
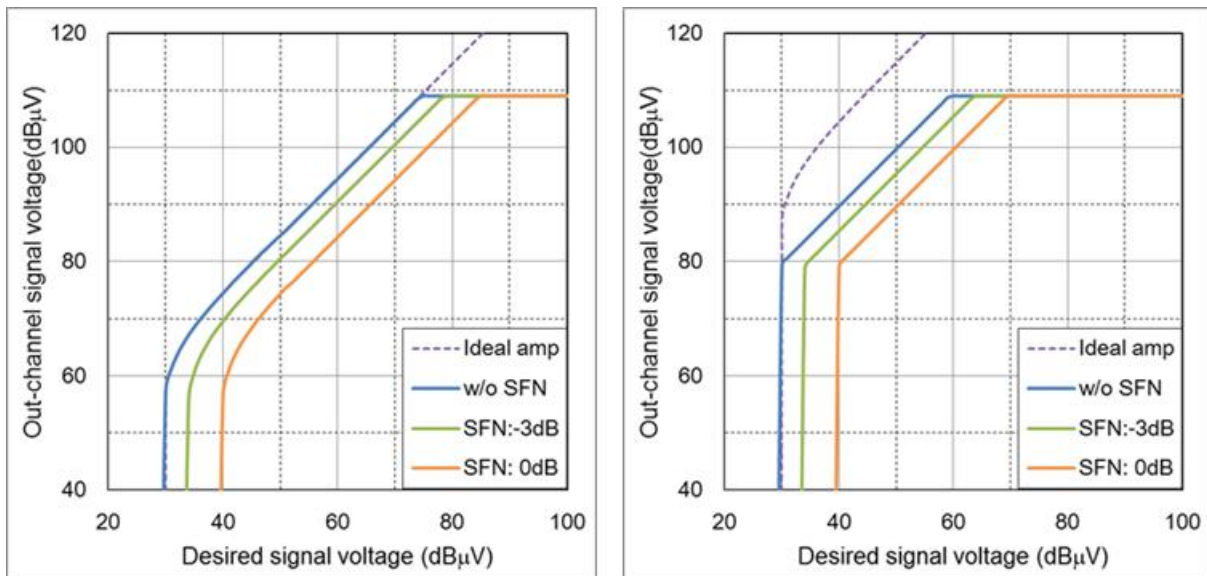
FIGURE 28

Unnecessary components and out-channel interference characteristics
(APN = –35 dB, R = 50 dB, X_{sat} = 0 dBm)
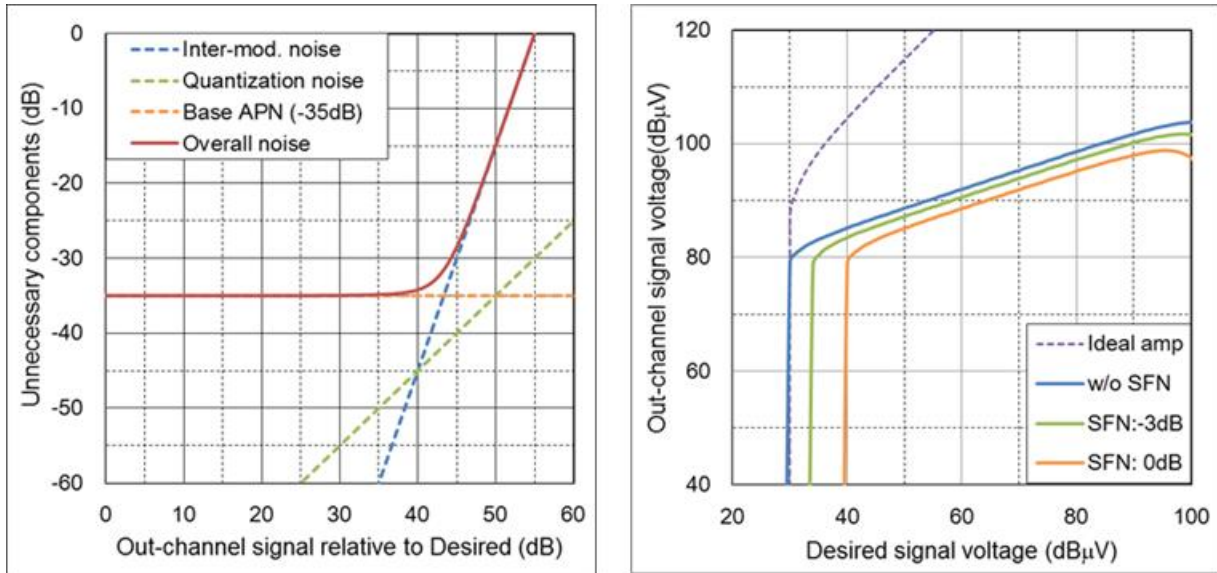
a) Unnecessary components

b) Out-channel interference characteristics

FIGURE 29

Out-channel interference characteristics with attenuator controlled

a) APN = –35 dB, R = 20 dB, X_{sat} = 0 dBm

b) APN = –35 dB, R = 50 dB, X_{sat} = 0 dBm

Taking these issues into consideration, the out-channel interference characteristics of a reference receiver should be specified on the 2-dimensional diagram, together with the specifications for APN, out-channel suppression ratio and intermodulation factor (or amplifier saturation level) so that the characteristics can be calculated for any SFN conditions.

4.4 Aliasing noise

The out-channel components being converted into the frequency band near the sampling frequency of A/D converter generate aliasing noise. The out-channel components are reduced by the IF filter and the frequency converted components are further reduced by the LPF accompanied with A/D converter. Adding the aliasing noise to equation (36), the overall unnecessary component is obtained by the following equation.

$$
\begin{aligned}
N_a &= LPF^{-1} \cdot U_a / R_a \\
N_{eq} &= N_{fix} + APN \cdot (D + U/R) + N_{im}(D + U)^3 + N_a
\end{aligned}
\tag{38}
$$

where

N_a :   denotes aliasing noise included in the desired signal

U_a :   power of out-channel components within the aliasing frequency band

R_a :   suppression ratio of the IF filter against the aliasing frequency band

LPF :   out-band attenuation of the LPF.

Chapter IV

Fading

Recommendation ITU-R P.1546 gives the relationship of reception field strength vs. propagation distance for various time availabilities. We assume here fading margins to be the difference between the field strengths of the designated time availability and that of 50% time (annual mean value). The Recommendation states that the data is valid for time availabilities only between 50% and 1%. For the range less than 1% of time, we assume the so-called Kumada's law, details of which are described in Appendix 1.

Figure 30 shows the fading margins derived from the above. The curves in the figure correspond to transmission antenna heights. Since these fading margins are derived from the Recommendation, general treatments, such as interpolation of time availability, antenna height, etc. are to follow the Recommendation.
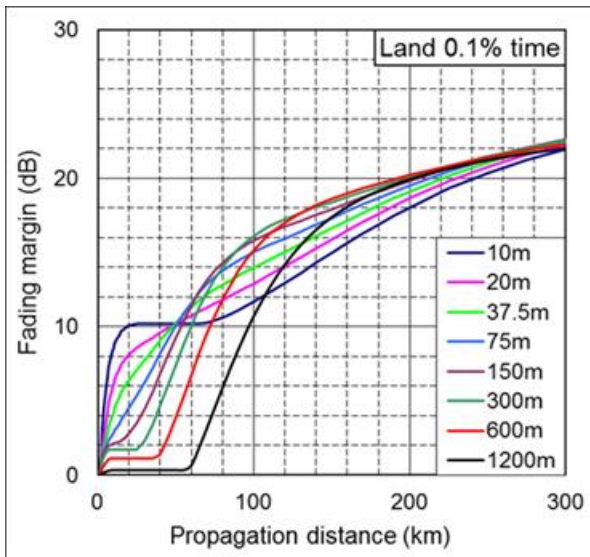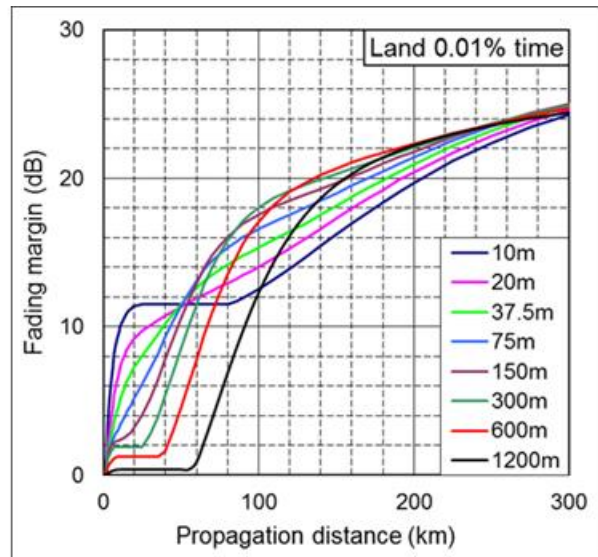
FIGURE 30

Fading margins (600 MHz)
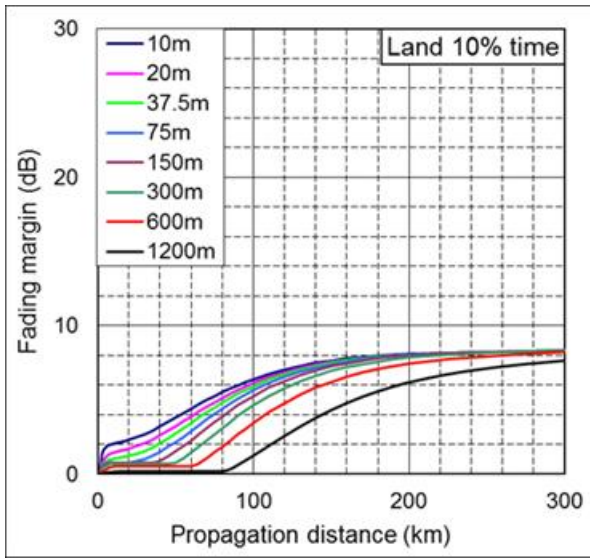
a) 10% of time (land path)
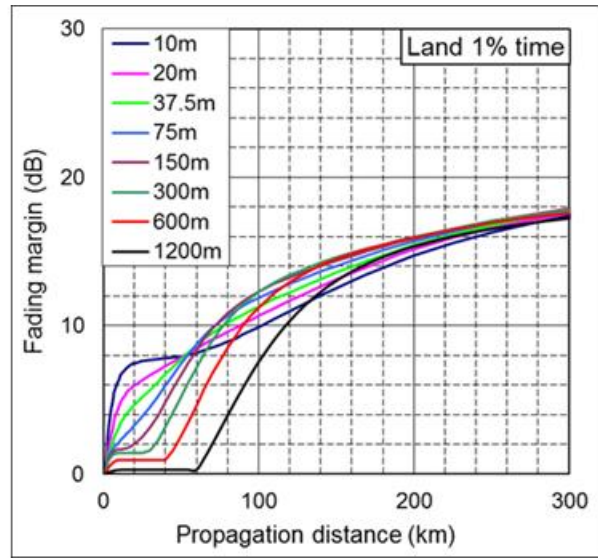
b) 1% of time (land path)

c) 0.1% of time (land path)

d) 0.01% of time (land path)

Appendix 1

## Fading margin for less than 1% of time (Kumada's law)

Figure 31 shows examples of measurement results of field strength coming from Korea to Japan. The analogue TV waves emitted at several cities in Korea were continuously measured for a one-year period. Figure 31a is the results measured during June and Fig. 31b during December. The field strengths present big changes in June while almost constant in December. In this area, fading phenomenon takes places very often during May to October and it is rarely during December to March.

FIGURE 31

Measurement examples of field strengths coming from Korea (sea path)
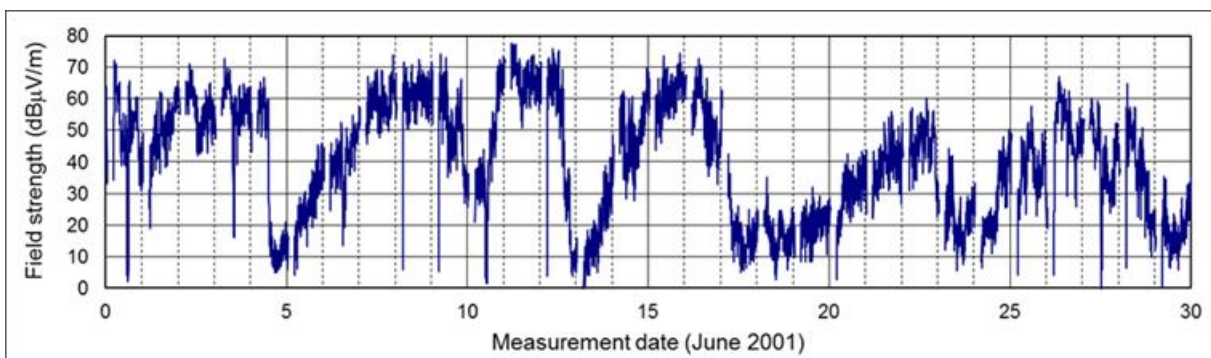

a) Fading season (June 2001)
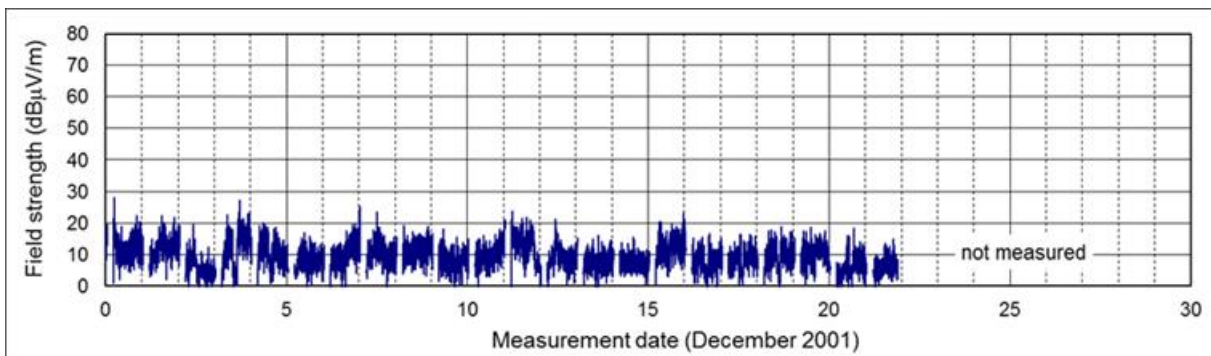
b) Non-fading season (December 2001)

Figure 32 shows the cumulative percentage of field strength measured in different places. Although the field strengths corresponding to a certain percentage of time are different by propagation distances, frequencies (channels), etc. we can see a common feature from the measurement results, as follows.

FIGURE 32

Cumulative percentage of field strengths coming from Korea (sea path)
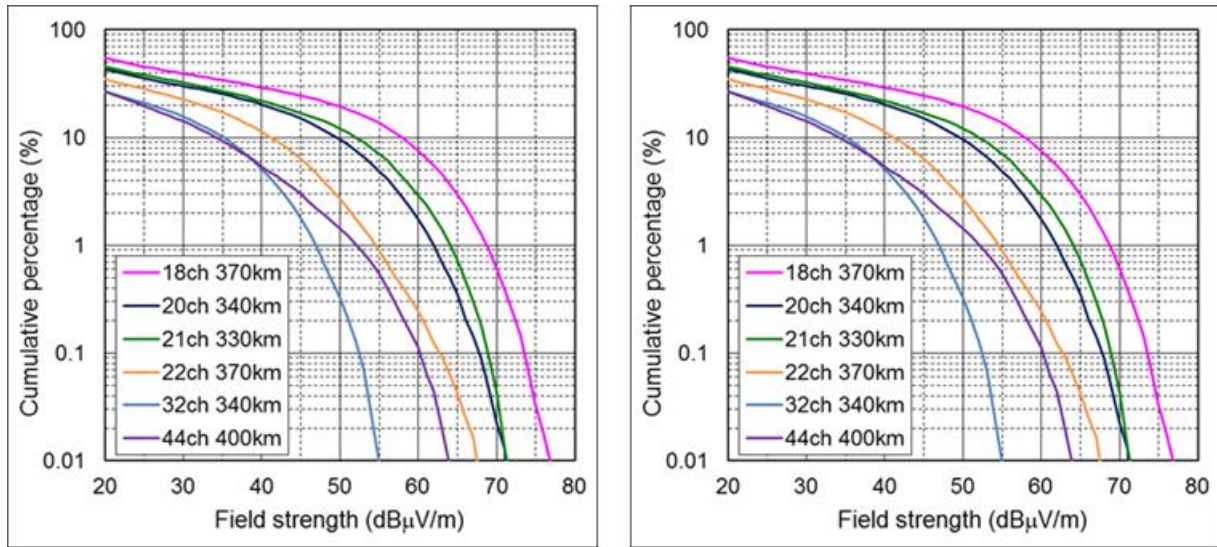
a) Measured at Nishino-shima　　　　　　　　　b) Measured at Toyokita

When the field strengths for 10% of time and 1% of time are to be FS_{10} and FS_1 (dB(μV/m)), respectively, the field strengths for 0.1% and for 0.01% of time can be obtained by the following equations.
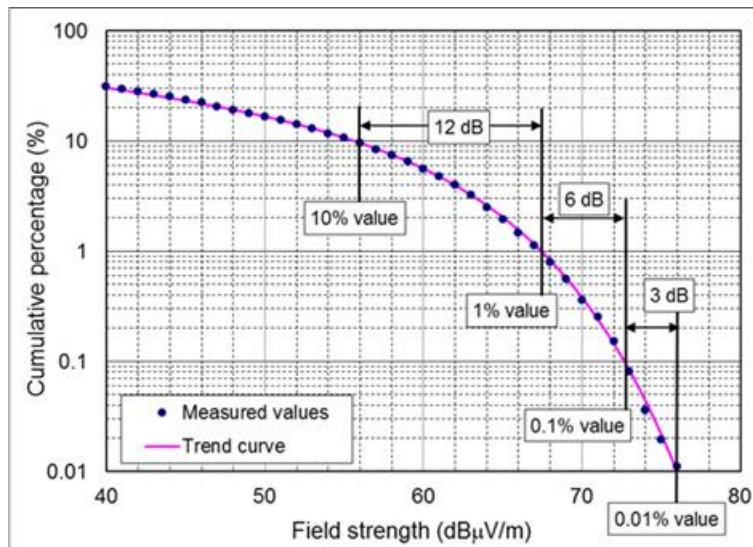
$$FS_{01} = FS_1 + \frac{1}{2}\left(FS_{10} - FS_1\right) \qquad \text{dB} \qquad (39)$$

$$FS_{001} = FS_{01} + \frac{1}{2}\left(FS_1 - FS_{01}\right) \qquad \text{dB} \qquad (40)$$

where, FS_{01} and FS_{001} represent the field strengths for 0.1% of time and 0.01% of time respectively. The above simple equations are so-called Kumada's law. An example of it is shown in Fig. 33.

FIGURE 33

Example of Kumada's law

Appendix 2

Intermodulation noise

A2.1 Formulas for intermodulation calculations

We define the input/output characteristics of the first stage amplifier as follows.

$$y = x - Bx^3 \quad \text{and} \quad B = 1/\left(3x_{sat}^2\right) \tag{41}$$

where, x_{sat} denotes the input level at which the amplifier just saturates.

We express the input signal as follows.

$$x = \sum_i A_i \cos \omega_i t \equiv \sum_i a_i \tag{42}$$

The intermodulation components are the 3rd power of the signal.

$$
\begin{aligned}
x^3 &= \sum_i a_i^3 + 3\sum_i \sum_{j \neq i} a_i^2 a_j + 6\sum_i \sum_{j>i} \sum_{k>j} a_i a_j a_k \\
&= \tfrac{1}{4} \sum_i A_i^3 \left[\cos 3\omega_i t + 3\cos \omega_i t \right] + \tfrac{3}{4} \sum_i \sum_{j \neq i} A_i^2 A_j \left[\cos\left(2\omega_i \pm \omega_j\right)t + 2\cos \omega_j t \right] \\
&\quad + \tfrac{6}{4} \sum \sum \sum A_i A_j A_k \cos\left(\omega_i \pm \omega_j \pm \omega_k\right)t
\end{aligned}
\tag{43}
$$

The above equation includes components that fall into the frequencies 3 times the signal band, and we will obtain the intermodulation noise by removing these components.

$$
\begin{aligned}
IM = \frac{B}{4}\Bigg\{ &3\sum_i A_i^3 \cos \omega_i t + 6\sum_i \sum_{j \neq i} A_i^2 A_j \cos \omega_j t + 3\sum_i \sum_{j \neq i} A_i^2 A_j \cos\left(2\omega_i - \omega_j\right)t \\
&+6\sum_i \sum_{j>i} \sum_{k>j} A_i A_j A_k \left[\cos\left(\omega_i + \omega_j - \omega_k\right)t + \cos\left(\omega_i - \omega_j + \omega_k\right)t + \cos\left(-\omega_i + \omega_j + \omega_k\right)t\right]\Bigg\}
\end{aligned}
\tag{44}
$$

Figure 34 shows calculation examples of the intermodulation noise of an OFDM signal. The horizontal axis denotes UHF channels and the vertical axis signal levels in dBμV/0.5 MHz. The green coloured bar and orange coloured curve in the graphics expresses the OFDM signal and the spectrum of intermodulation noise, respectively. The figure at the top-left corner of each graph expresses the intermodulation noise that falls into the OFDM signal band. The amplifier used in the calculation has a saturation level of x_{sat} = 109 dBμV (0 dBm).

Figures 34a, 34b and 34c are for the signal levels of 60 dBμV, 80 dBμV and 100 dBμV, respectively. Note that the graphics are displayed by approximately 10 dB lower than the signal levels indicated in the captions, as they are expressed in spectrum per 0.5 MHz while the captions are expressed for the signal bandwidth of 5.6 MHz. It is seen from the figure that the intermodulation noise increases at a rate of 30 dB/decade.

FIGURE 34

Signal level vs. intermodulation noise
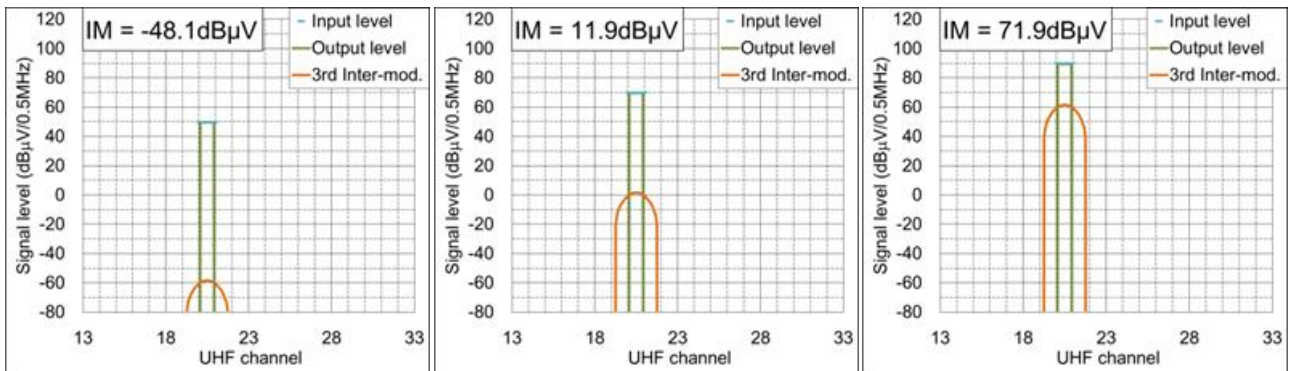
a) Signal level = 60 dBμV   b) Signal level = 80 dBμV   c) Signal level = 100 dBμV

A2.2 Examples of intermodulation noise

Figure 35 shows examples of intermodulation noise for various undesired channels. Figures 35a to 35c show the case of adjacent channel, in which channel #20 is the desired signal at 60 dBμV and #21 is the adjacent channel undesired signal. In this case, the side lobe of intermodulation components around the undesired channel overlaps with the desired channel, resulting in a large noise on the desired signal.

Figures 35d to 35f show the case of 2nd adjacent channel (#22). In this case, the side lobe around the undesired channel does not overlap with the desired channel, resulting in a relatively small noise on the desired channel.

Figures 35g to 35i show the case of 10 undesired channels (#22-#31), where each undesired signal is reduced by 10 dB in order to maintain the total power of undesired signals being the same as that in the other graphs, i.e. 60 dBμV, 80 dBμV and 100 dBμV. In this case, the intermodulation components spread widely over the channels, resulting in a relatively large noise on the desired signal.
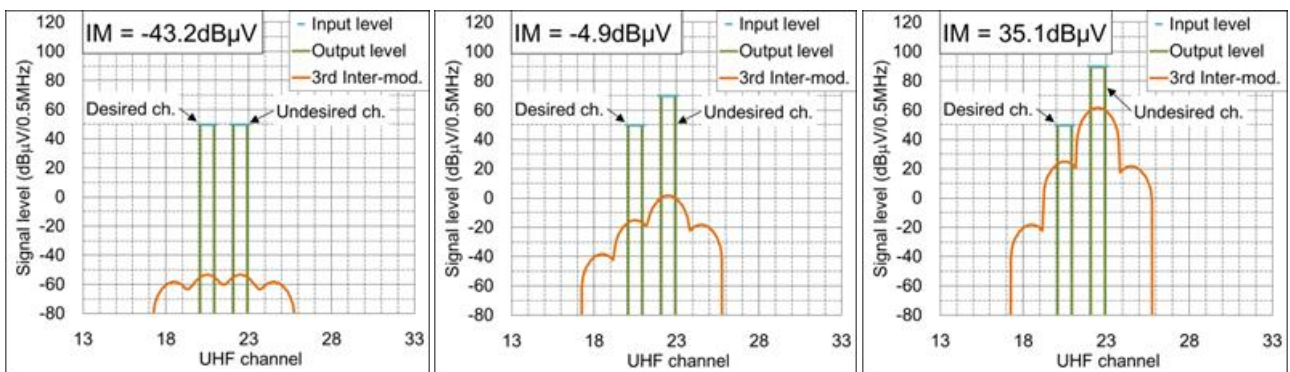
FIGURE 35

Dependency of intermodulation noise by channels, etc.
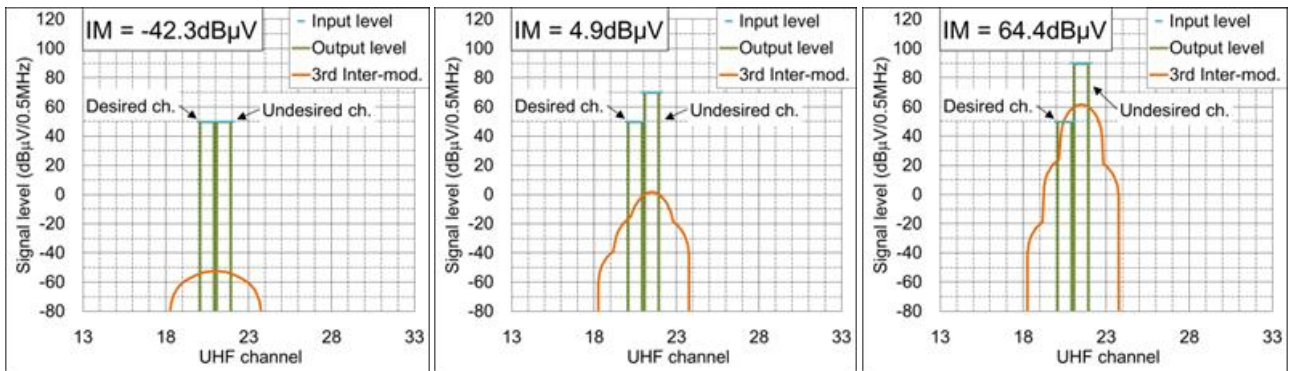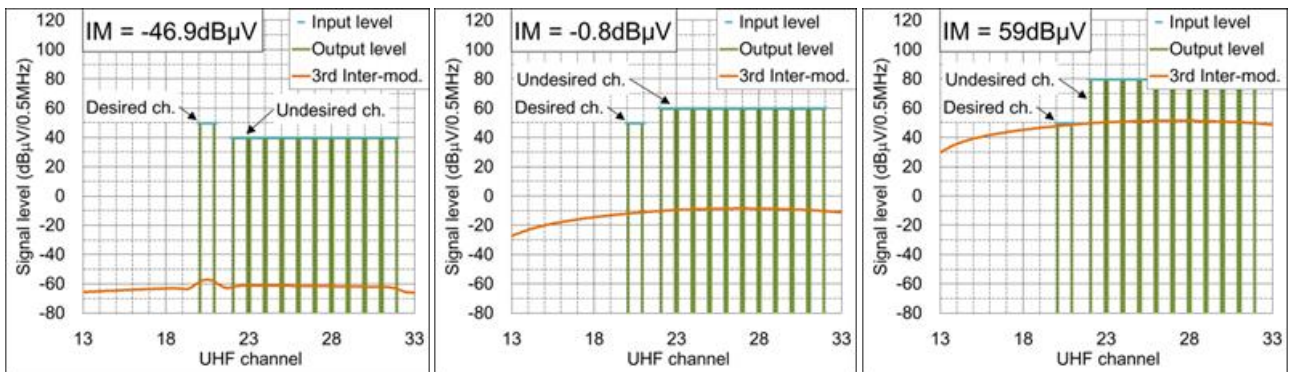

a) Adj. channel = 60 dBμV

b) Adj. channel = 80 dBμV

c) Adj. channel = 100 dBμV

d) 2nd Adj. channel = 60 dBμV

e) 2nd Adj. channel = 80 dBμV

f) 2nd Adj. channel = 100 dBμV

g) 10 channels = 60 dBμV

h) 10 channels = 80 dBμV

i) 10 channels = 100 dBμV

A2.3   Determination of coefficient N_{im}

Figure 36 shows the relationship between intermodulation noise and signal levels for various conditions.

The dot line (denoted by "Intermodulation") in the graphics is for the case without undesired signals, corresponding to Fig. 34. The intermodulation noise increases in proportion to the 3rd power of signal level (increase rate of 30 dB/decade).

The orange coloured curve ("1st Adj. channel") is for the case of adjacent channel, corresponding to Figs 35a to 35c. The noise takes a constant value at low undesired signal levels, which corresponds to the intermodulation noise generated solely by the desired signal, while it increases in proportion to the 3rd power of undesired signal level (30 dB/decade) in the range higher than the desired signal (60 dBμV).

The green colour curve ("2nd Adj. channel") is for the case of 2nd adjacent channel, corresponding to Figs 35d to 35f. The noise increases in proportion to the 2nd power of undesired signal (20 dB/decade), which differs from the other cases of the 3rd power (30 dB/decade).

The dark purple coloured curve ("10 channels") is for the case of 10 undesired channels, corresponding to Figs 35g to 35i. The noise increases in proportion to the 3rd power of undesired signal (30 dB/decade).

The intermodulation noise thus varies by the number of out-channel undesired signals and/or frequency separation even if the out-channel signal power is the same. We will choose the adjacent channel case to be applied in the interference calculation, because the condition generates the most severe intermodulation noise. In this case, the intermodulation noise is calculated to be 17 dB lower than the amplifier saturation level when the input signal is at the saturation level (x_{sat}). Then the value of coefficient N_{im} applied in equations (36), etc. is obtained as follows.

$$N_{im} = 1/\left(50 x_{sat}^2\right) \quad \text{or} \quad N_{im}(\text{dB}) = -2 \times x_{sat}(\text{dB}) - 17(\text{dB}) \tag{45}$$

FIGURE 36

Signal level vs. intermodulation noise